

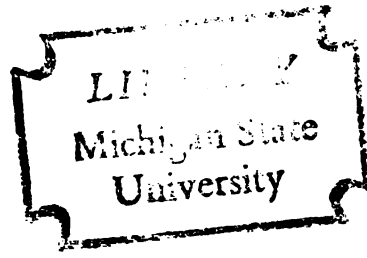
KINETICS OF CONTINUOUS PRECIPITATION IN A DILUTE
SYSTEM; MAGNESIUM HYDROXIDE

Thesis for the Degree of M. S.
MICHIGAN STATE UNIVERSITY

PHILIP B. HARTWICK

1975

122218



6193650

ABSTRACT

KINETICS OF CONTINUOUS PRECIPITATION IN A DILUTE SYSTEM; MAGNESIUM HYDROXIDE

By

Philip B. Hartwick

This study constitutes the second step of a program attempting to model the removal of dilute impurities from water streams using precipitation, agglomeration, and flocculation. The lime-soda ash process currently being used in many municipal water softening plants was the process under investigation. This process is also being looked at as a probable component of total recycle in industrial cooling water systems. In a previous study, it was shown that the water softening process can be partially described using crystal nucleation and growth kinetics.

This research investigates the kinetics of precipitation of magnesium hydroxide. Crystal size distribution (CSD) in a continuous backmix reactor at various residence times was determined as a function of supersaturation. McCabe's ΔL law (size independent crystal growth) was found to apply, so that population balance theory could be used to describe the CSD. Nucleation

and growth rates were determined as a function of magnesium and hydroxide concentrations at 25°C.

B^0 = nucleation rate (nuclei per minute per ml)

$$B^0 = 3.95 \times 10^{12} (C_{OH}^2 C_{Mg} - 6.95 \times 10^{-10})$$

G = growth rate (microns per minute)

$$G = 3.83 \times 10^5 (C_{OH} C_{Mg} - 2.97 \times 10^{-8})$$

In the light of these findings, several design changes to improve the separation process are recommended:

1. Larger rapid mix volume.
2. Diversion of some of the slaked lime feed to the flocculation basins.
3. Recycle of primary sludge in systems where this is not already practiced.

The first two suggestions would decrease operating hydroxide concentrations in the rapid mix area, resulting in lower nucleation rates and, as an end result, a higher solid fraction in the sludge. Primary sludge recycle would have the same effect, while increasing the surface area for deposition to maintain the quality of the treated water.

Further investigations with the mixed precipitations, characteristic of lime-soda systems, are necessary to verify the above recommendations.

KINETICS OF CONTINUOUS PRECIPITATION IN A
DILUTE SYSTEM; MAGNESIUM HYDROXIDE

By

Philip B. Hartwick

A THESIS

Submitted to
Michigan State University
in partial fulfillment of the requirements
for the degree of

MASTER OF SCIENCE

Department of Chemical Engineering

1975

This work is dedicated to
all people who drink water.

ACKNOWLEDGMENTS

I would like to thank all those who in any way helped me further my studies so that I might now attempt to further the science of water purification. In particular I would like to thank my Professor, P. M. Schierholz, for introducing me to the field of particulate processes and guiding my investigation; my wife Tracey for stabilizing my existence and sharpening my tone; and my assistant, G. R. Bailie, whose companionship and effort helped get the data in.

TABLE OF CONTENTS

	Page
LIST OF TABLES	v
LIST OF FIGURES	vi
NOMENCLATURE	viii
 INTRODUCTION	 1
BACKGROUND	4
Kinetics Determination	7
Lime-Soda Water Softening	8
The Problem	14
 EXPERIMENTAL	 15
RESULTS	25
DISCUSSION	44
CONCLUSIONS	57
RECOMMENDATIONS	59
Lime-Soda Ash Water Softening	59
Lime-Soda Ash Modeling Study	59
 Appendices	 60
A. A PROGRAM FOR FITTING COUNTS TO THE SIZE INDEPENDENT GROWTH MODEL	61
B. METHODS OF MAGNESIUM AND HYDROXIDE ANALYSIS	65
C. DATA AVERAGING	69
 BIBLIOGRAPHY	 76

LIST OF TABLES

Table	Page
1. Results from material balance	27
2. Results from crystal size distribution	28

LIST OF FIGURES

Figure	Page
1. Lansing water softening process	10
2. Mini-plant for precipitation studies	16
3. Crystallizer less feed and withdrawal tubes	18
4. Bail and beaker sampler	21
5. Equipment list and manufacturers	23
6. Typical crystal size distribution	26
7. Solid crystal with a clump of small flake aggregates	30
8. Detail of Figure 7, edge shot of star aggregate	30
9. Crystal flakes and aggregates, thin edge	32
10. Unusual "sponge" crystal formed at 20 minute residence time, Run 6-3	32
11. Solid crystal, fairly common at longer residence times, Run 6-3	34
12. Unusual hollow "needle" crystal, Run 6-3	34
13. Detail of Figure 12, point of needle crystal	36
14. Large solid crystal, plate-like appearance, Run 5-15	36
15. Large clump of flake aggregates, most com- monly seen crystals in the laboratory samples, predominant at shorter resi- dence times, Run 5-15	38
16. Agglomerate taken after the rapid mix area of the Lansing drinking water treatment plant, representative formation	38

Figure	Page
17. Layered finger, representative of sample taken after the rapid mix	40
18. Representative agglomerates from the first flocculation basin	40
19. Representative agglomerate from the third flocculation basin	42
20. Representative agglomerate from the fifth and last flocculation basin	42
21. Film theory for magnesium hydroxide growth	45
22. Film theory for induction of high ionic strength near a growing crystal	47
23. Nucleation rate as a function of reactant concentrations	50
24. Growth rate as a function of reactant concentrations	51
25. Growth rate versus $C_{Mg} C_{OH}^2$	52
26. Nucleation rate versus $C_{Mg} C_{OH}$	53

NOMENCLATURE

<u>Symbol</u>	<u>Description</u>
B^0	Nuclei birth rate, numbers per milliliter per minute.
C_{Mg}	Magnesium concentration, equivalents per liter.
C_{OH}	Hydroxide concentration, equivalents per liter.
G	Crystal growth rate, microns per minute.
K_g	Growth constant.
K_n	Nucleation constant.
k_v	Shape factor, for a sphere $\pi/6$, this was the value used in this study.
L	The characteristic dimension of a particle, determined by the increase in resistance across an aperture with an electrolyte moving through when a particle is present. Reported as an equivalent spherical diameter, microns.
M_{T1}	Suspension density calculated from material balance, grams of crystals per liter of solution.
M_{T2}	Suspension density calculated from the crystal size distribution, grams of crystals per liter of solution.
n	Particle density, expressed as a function of L , numbers per milliliter per micron.
n^0	Nuclei density, the particle density at $L = 0$, numbers per milliliter per micron.
R_{Mg}	Rate of make of magnesium into crystals, calculated from the material balance, equivalents per minute.
R_{OH}	Rate of make of hydroxide into crystals, calculated from the material balance, equivalents per minute.

<u>Symbol</u>	<u>Description</u>
ρ	Crystal density, taken as literature value for stable crystals.
s	Supersaturation, solution concentration less equilibrium concentration.
s_g	Growth supersaturation, an experimentally determined expression.
s_n	Nucleation supersaturation, an experimentally determined expression.
τ	Mean residence time in the crystallizer, minutes.
u_t	Free settling velocity (terminal velocity) of a particle moving through a fluid due to gravitational force.
V	Average volume of crystallizer.

INTRODUCTION

The lime-soda ash system has been used extensively to improve the quality of municipal water supply. The process has been studied rather extensively; indeed, the Journal of the American Water Works Association regularly delves into its murky waters. A school of thought, of independent origin, with roots in Tucson and Ames, dealing in analysis and techniques of continuous crystallization, has presumed to challenge the aged knowledge of the AWWA. The proof, of course, is in the pudding. Can the system be improved upon?

The primary tool of these upstarts is kinetic studies; growth and nucleation rates are related to each other and to supersaturation. P. M. Schierholz (25) kicked off the attack on lime-soda ash water softening by determining relationships between nucleation and growth for calcium carbonate precipitation. In this project magnesium hydroxide precipitation was considered. Between the two, the predominant constituents of water hardness were individually scrutinized.

The necessity for a clearer picture of lime-soda ash water softening becomes apparent when considered in the context of the ecology movement in this country.

Public outcry against pollution in the strident sixties resulted in the Federal Water Pollution Control Act of 1972, one result of which is an accelerating trend towards water recycle in a broad spectrum of industrial application. For example: cooling water is often recooled by evaporation for reuse, with blow down water being bled off and replaced with fresh water, to keep ionic levels out of the supersaturation range, preventing scaling of heat exchange equipment. Elimination of blow down necessitates an alternative method of hardness control. A current study by Hartline (12) indicates that the lime-soda ash process is preferred. Unfortunately, application to a recycle system brings up problems not evident in a once-through system like municipal water supply. For instance, in present practice polyphosphates are added to the treated water prior to sand filtration to eliminate further deposition of crystals on the filter sand. This would likely have a ruinous effect on the precipitation reaction in a recycle system. Polyphosphates are also added to cooling water to reduce scaling, compounding the problem. If by improving the efficiency of the precipitation process, operating hardness levels could be economically reduced to a point where scaling was no longer a problem, then polyphosphates could be eliminated from the system.

The goal of this series of investigations is economical and operational improvement in the lime-soda ash water softening process. Under the conditions of low suspension density, short residence times and small crystal size distribution, the phenomena of crystal growth and nucleation were isolated and modeled for magnesium hydroxide precipitation in the absence of other precipitating compounds. Techniques employed with success by Randolph and Larson (22) on concentrated systems and adapted by Schierholz and Stevens (26) to dilute systems were used in evaluation of crystal size distribution.

BACKGROUND

The problem of characterizing a population of particles produced in a system is not a simple one. If the system involves the formation of particles of a single habit (characteristic shape) then a particle of a given size can be formed by three mechanisms: growth --a smaller particle can grow by solute deposition; attrition--a larger particle can break due to mechanical action; and agglomeration--smaller particles can come together forming a larger one. A fourth mechanism, flocculation, occurs when a flocculating agent tends to sweep other particles out of suspension, forming a much larger aggregate. Magnesium hydroxide is considered to be a flocculating agent in lime-soda water softening (31). In a flow system with no crystals in the feed, yet another mechanism may occur, nucleation--the birth of very small crystals. The picture is simplified considerably if the crystals do not interact with one another or with the crystallization vessel, in which case the crystals don't break (attrition) or stick together (agglomeration and flocculation). Under this assumption, nucleation and growth are the only means by which a particular size may be reached. The no interaction

condition is approached in dilute slurries with short residence times.

The driving force for precipitation, supersaturation, has been defined by Mullin (19) as the difference between solute concentration and equilibrium concentration. Unfortunately, most systems investigated in the past have involved immeasurably low levels of supersaturation. Temperature difference in cooling crystallizers has been used as a measure of supersaturation. Ideally, the kinetic parameters (nucleation and growth) should be modeled in terms of the concentrations of the reacting species for isothermal crystallization (22). In dilute systems relative supersaturations are much higher than in most concentrated systems studied in the past, raising the hope that results from this investigation can correlate supersaturation with nucleation and growth rates. The traditional definition of supersaturation lacks generality when there are more than one reacting species. A general model cannot assume stoichiometric ratios or constant concentration of one of the reactants. The definition of supersaturation should be modified to apply to ionic precipitation reactions.

It has been shown that new crystal formation can result from homogeneous nucleation, heterogeneous nucleation, and secondary nucleation. Homogeneous nucleation

is the formation of a new crystal from the liquid phase as a result of supersaturation alone. Heterogeneous nucleation normally involves new crystals formed around minute foreign material. The foreign particles provide sites for deposition with reduced energy requirements. Secondary nucleation is thought to involve crystals bumping into one another creating nuclei. Randolph and Larson (22) model secondary nucleation rate as proportional to the mass of solids in suspension. In light suspensions secondary nucleation should not be an important factor. Homogeneous nucleation has been reported for magnesium hydroxide in batch studies (16) with nucleation rate dependent on $(C_{Mg} \times C_{OH}^2)^{33}$ at supersaturation ratios as low as four. In other batch studies, Gunn and Murthy (11) reported induction times in terms of concentrations: $\Delta t \text{ (sec)} = 1.389 \times 10^{-15} (C_{Mg} C_{OH}^2)^{-1.85}$. When the ionic reactants are mixed together in a supersaturated condition nuclei may eventually appear. The time interval between mixing and the appearance of crystals is known as the induction period. The relation between induction period in batch studies and nucleation rate in continuous systems is rather obtuse, but some correlation should exist.

Growth rates for magnesium hydroxide crystals are not reported in the literature. Schierholz (25) in his investigation of calcium carbonate reported growth

rates but found no correlation to reactant concentration. It is well known that for small crystals (less than five microns) growth rate depends on size (19). Randolph and Larson (22) mention that for most highly hydrated crystals growth is a function of size, with alum as an exception. Magnesium hydroxide is known to be a highly hydrated crystal (19). The McCabe ΔL law states that growth rate is independent of size. For crystals larger than a few microns this has been found to often be the case (22, 25).

Kinetics Determination

A mixed suspension mixed product removal (MSMPR) crystallizer was used to determine the kinetics of magnesium hydroxide precipitation. Population balance theory (Randolph and Larson, 22) was applied to express the crystal size distribution in terms of nuclei density, growth rate and mean residence time. Assuming steady state, no crystals in the feed, no attrition, agglomeration or flocculation, no classification of withdrawal, perfect mixing, and growth rate independent of size, application of a population balance results in,

$$\frac{dn}{dL} + \frac{n}{G\tau} = 0 .$$

Solution of the differential equation yields,

$$n = n^0 \exp (-L/G\tau) ,$$

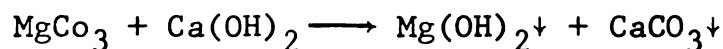
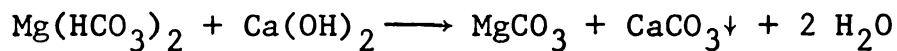
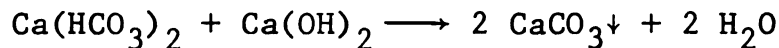
where n is the particle density of crystals with a characteristic dimension L , G is the crystal growth rate and τ is the mean residence time. The nucleation rate may be expressed as,

$$B^0 = n^0 G .$$

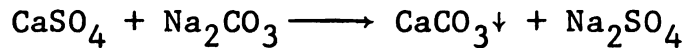
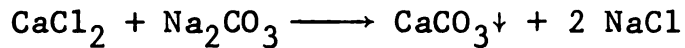
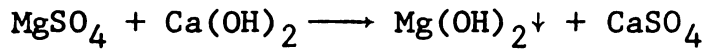
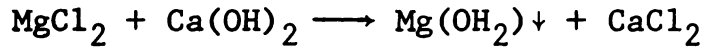
Lime-Soda Water Softening

Water taken from wells or streams is often softened before distribution. Hard water is water containing objectionable amounts of dissolved salts of calcium and magnesium. In large municipal systems, the raw water is softened via a lime-soda ash or lime process to a finished product containing 1.6-2.4 mg/l of magnesium and calcium.

The two types of water hardness are carbonate (temporary) and noncarbonate (permanent). Temporary hardness, calcium and magnesium bicarbonate, is removed by the addition of lime, resulting in the precipitation of calcium carbonate and magnesium hydroxide. The reactions in lime treatment are:



Noncarbonate hardness is removed by addition of lime and soda ash. The additional reactions for lime-soda ash treatment are:



Two schemes of lime-soda water softening are currently in use. Split treatment is represented by Lansing's water softening facilities while Dayton often uses only lime softening in a one-shot system.

The following description of split treatment is based on the Lansing and Dayton systems. Lansing's system is diagrammed schematically in Figure 1. Dayton's system follows a similar flow chart with a different physical configuration.

Rapid Mix

Quick lime (CaO) is slaked with water in the chemical feeder to form calcium hydroxide. The slaked lime is then added to about 80 percent of the raw well water in the rapid mixer. One equivalent of lime is required for each equivalent of calcium while two are

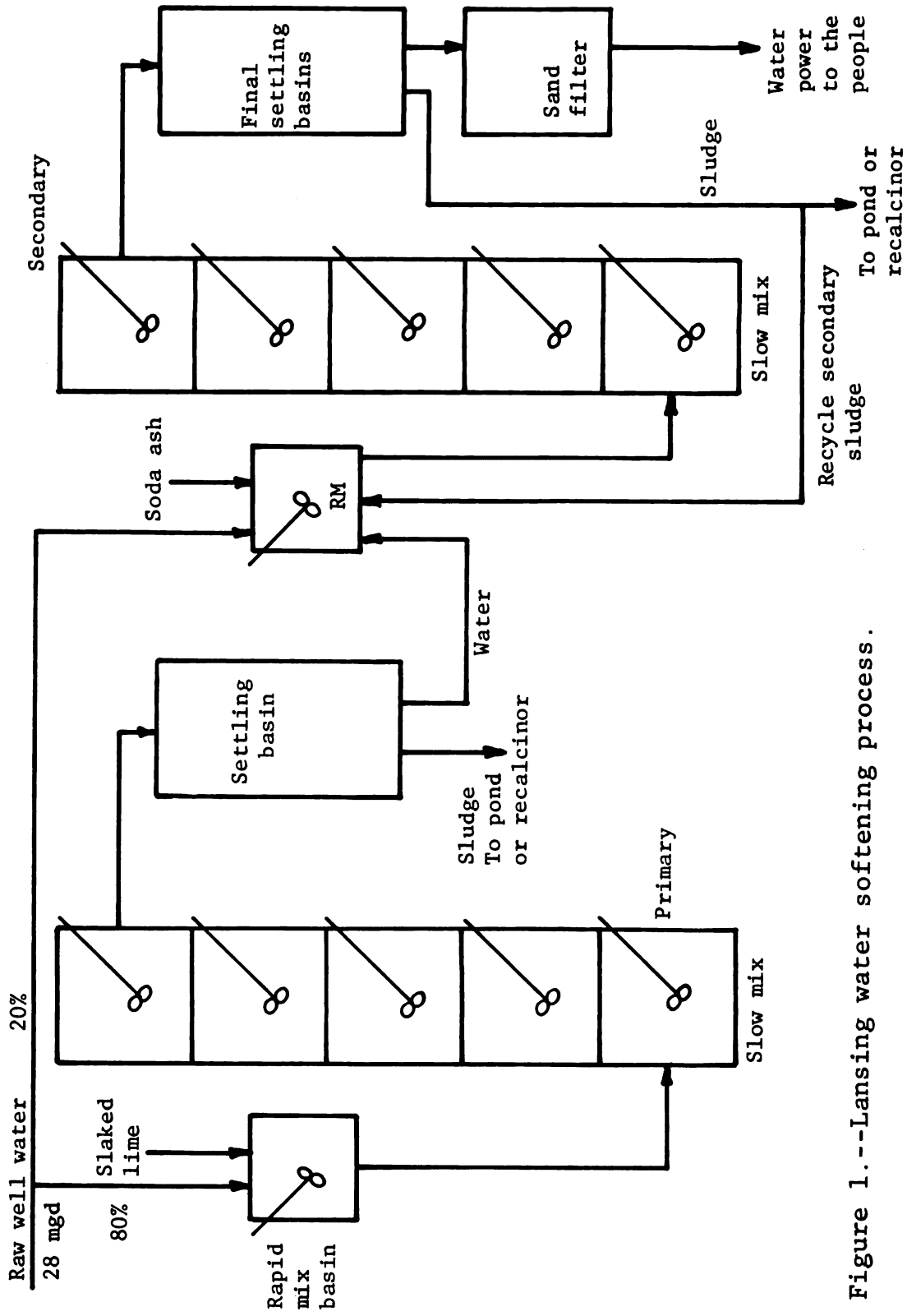


Figure 1.--Lansing water softening process.

required for each equivalent of magnesium. Excess lime is added to drive the reactions.

Flocculation

In the series of flocculation chambers the reactants are given time to take the precipitation toward equilibrium. Nucleation, growth, agglomeration and flocculation are thought to take place here. The magnesium hydroxide acts as a flocculating agent facilitating the removal of fine calcium carbonate crystals (31).

Primary Settling

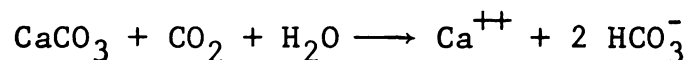
The purpose of the settling basis is to separate the fine crystalline materials from the water. No agitation is used and the crystals sink to the bottom where scrapers take them to a sludge sump.

Carbonation

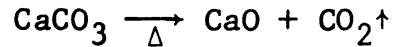
If a once-through system is used the excess lime can be neutralized by bubbling carbon dioxide gas through the water:



Any excess carbon dioxide is likely to dissolve calcium carbonate:



The carbon dioxide is normally available from the recalciner where the sludge is fired to reform the quick lime used in treatment:



At Dayton, one-pass primary treatment with carbonation is used when part of the system is down for maintenance. Back-up underwater burners are in place to supply CO_2 should the recalcining kiln be down.

Secondary Rapid Mix

Here water from the primary settling basis, by-passed raw water from the wells, soda ash and recirculated secondary sludge are mixed. The soda ash precipitates noncarbonate hardness and the recycled secondary sludge facilitates formation of large crystals as well as providing surface area for deposition.

Following secondary rapid mix are flocculation and settling chambers much the same as in primary treatment with an additional settling chamber to reduce fine crystals in the water prior to filtration and distribution to the customer.

The sludge is either dewatered, recalcined and used as quick lime or diverted to a disposal pond where it slowly dries and compacts.

Design considerations are multifaceted. In Lansing the primary flocculating chambers have recently been modified to facilitate the movement of crystalline floc from one to another. This was accomplished by moving the connecting slots from midway up the walls dividing the flocculation basins to the bottom of the walls. The motive was to reduce crystalline buildup on the agitators by reducing suspension density. This move did reduce maintenance costs. However, reducing suspension density is counter to literature recommendations (14, 22) which suggest sludge recycle to improve sludge settling characteristics by increasing suspension density. Sludge in the Lansing plant has taken a turn for the worse since the modifications. Previously, 15 percent solids was not uncommon; presently, 10 percent solids is normal. The result is a 20 ton per day calcining plant can only produce 16 tons of quick lime daily. The economic trade-off is a net loss. Sludge recycle at Dayton is profitably being used in the primary rapid mix area resulting in high suspension density and higher sludge solid compositions (30). At Dayton the soda ash is added in the primary rapid mix rather than the secondary. This practice seems reasonable because the pH is higher in the primary system: high enough to keep all of the CO_2 in the carbonate form. In Dayton the secondary rapid mix basin mixes the water from the

primary with by-pass water, secondary sludge, and potato starch; a flocculant.

The Problem

The experimental phase of this investigation focused on the kinetics of precipitation of magnesium hydroxide in a (MSMPR) crystallizer. The mathematical tool used is the population balance. This is in addition to the traditional chemical engineering practice of using material and energy balances to characterize separation processes. The purpose of the experiments was to determine the nucleation and growth rates at various residence times and reactant concentrations, the ultimate objective being to determine nucleation and growth rates as a function of reactant concentrations. Temperature is also recognized as an important parameter; however, all experiments were conducted at 25°C. The use of various residence times served as an indication of the generality of the kinetic data obtained.

EXPERIMENTAL

A series of experiments were conducted in a mixed suspension mixed product removal (MSMPR) crystallizer system, assembled by the author. Previous systems described by Schierholz (25) and Randolph and Larson (22) were used as guides. Experience also became a guide. The system described in the following discussion is diagrammed in Figure 2. Feed solutions were made using distilled water. A solution of magnesium chloride was held in the Mg reservoir, and a solution of sodium hydroxide was held in the OH reservoir. Crystallizer concentrations were intended to range around those encountered in lime softening. Without knowing the kinetics of precipitation, the concentrations in the crystallizer could not be determined from the feed concentrations, making crystallizer concentration prediction an iterative process from one run to the next.

A styrofoam float in each reservoir suspended a cooling coil consisting of tygon tubing wrapped around a stainless steel frame with tap water as a coolant. Also on the float was a Haake temperature controller set at 25°C. Two rotary pumps supplied water to constant head tanks, by way of two wrapped string 5 micron

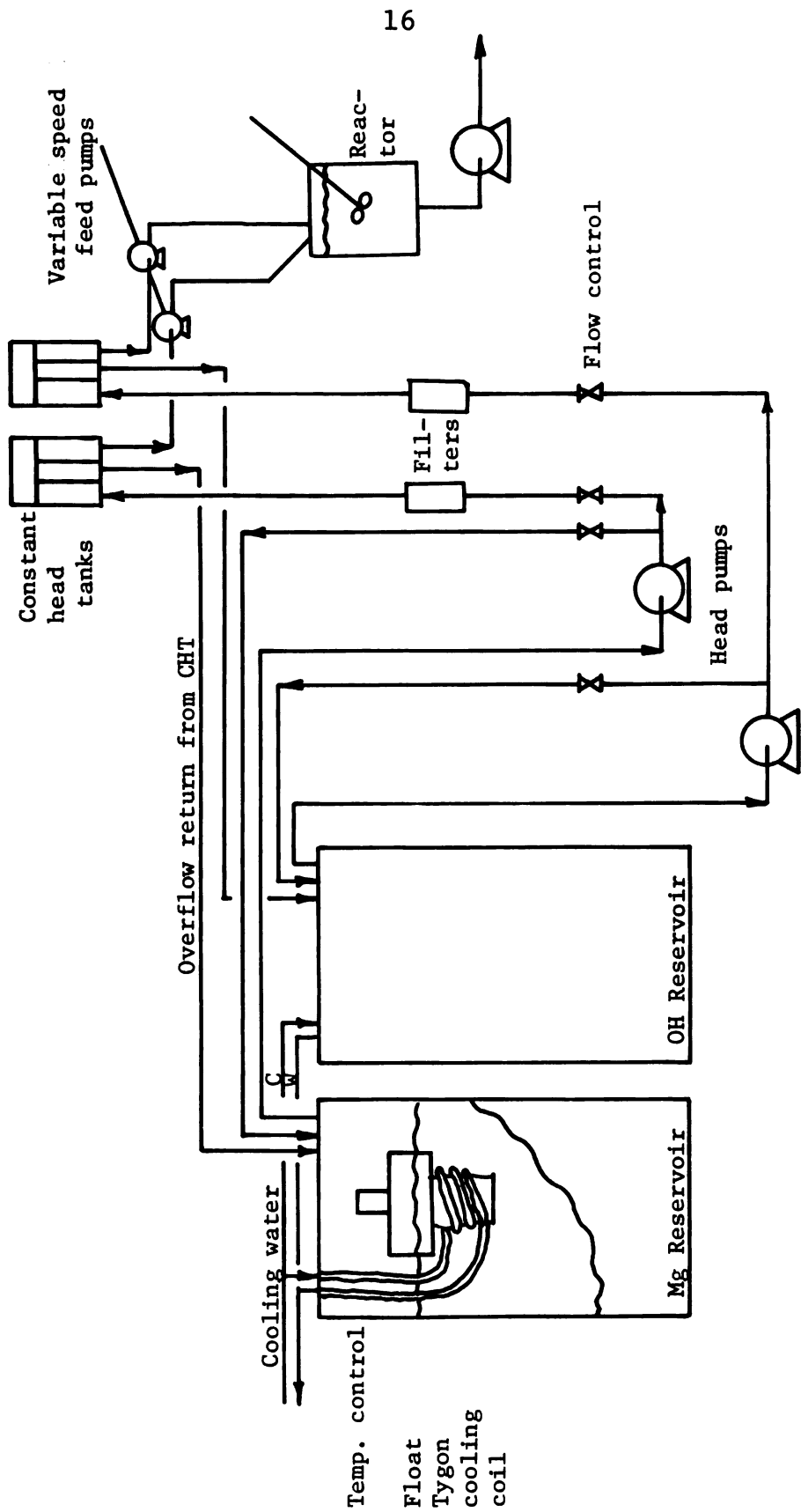


Figure 2.--Mini-plant for precipitation studies.

filters. Since the filters were rated for flow rates of 50 gallons per minute and used at rates around .04 gallons per minute the author presumes that only very small particles could be swept through the filter. The feed pumps consisted of two tandem peristaltic pumps driven by an 1800 rpm motor. Flow rates were measured at the beginning and end of each run with a 250 ml volumetric flask and a timer. Often no measurable difference was found. Residence time was varied between 8, 12 and 20 minutes by use of an adjustable gear reducer between the motor and the feed pumps.

The crystallizer is diagrammed in Figure 3. To prevent crystal build-up on the reactor surfaces all inside parts were scraped every five minutes with a rubber spatula. In runs where the crystallizer was not scraped, steady state in the crystal size distribution and the reactant concentrations was not obtainable. Baffles and draft tube are considered essential for complete mixing in high suspension density systems. They were not used in this system to minimize area for deposition, and to facilitate scraping. In this low suspension density system they seemed to be dispensable. To obtain isothermal conditions the room temperature was maintained at 25°C. Crystallizer temperature varied between 24.9 and 25.1°C. An agitator speed of 500 rpm was used in all cases. Withdrawal was accomplished

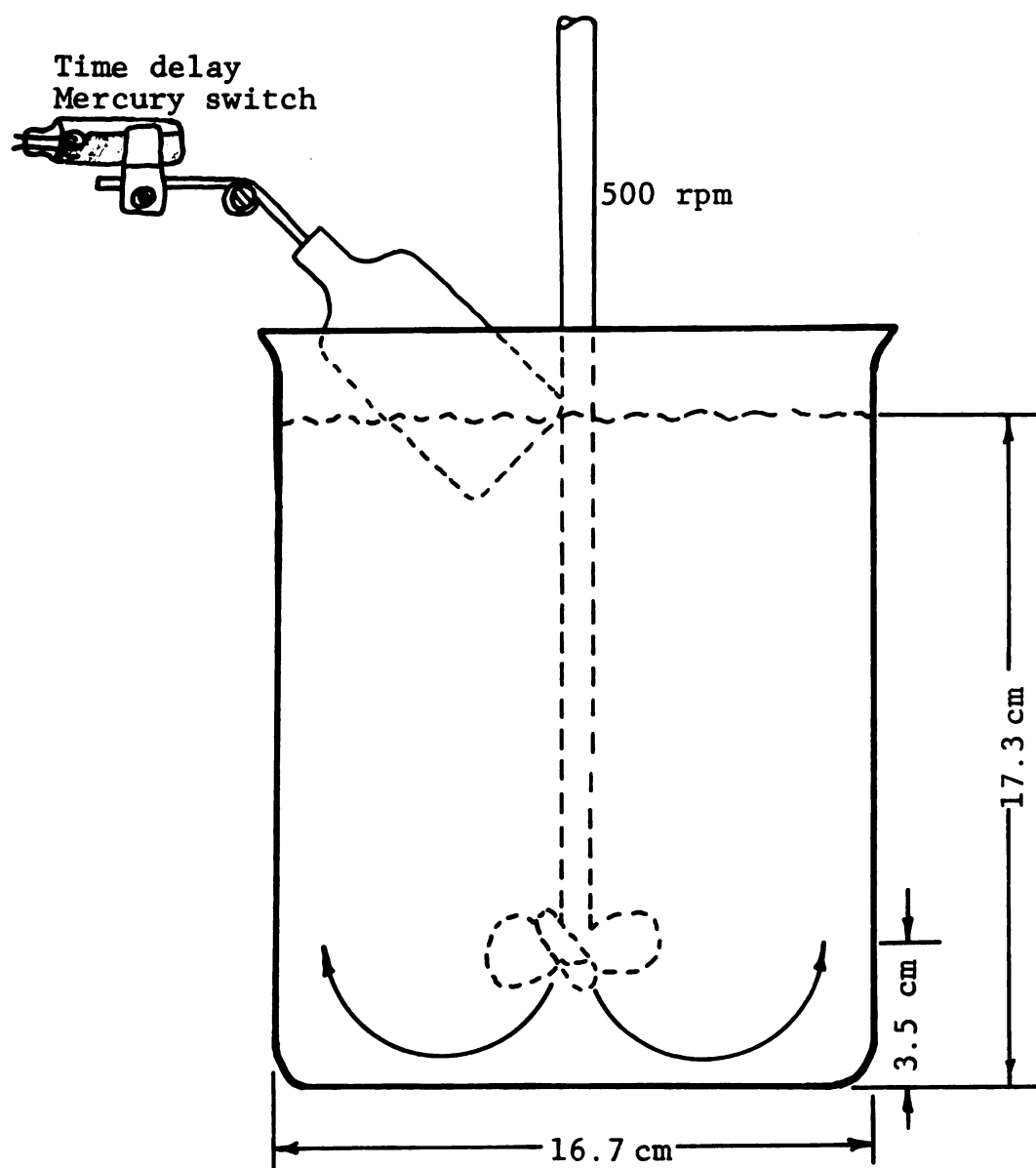


Figure 3.--Crystallizer less feed and withdrawal tubes.

intermittently using a float and a mercury switch to activate a pump. Each withdrawal pulse removed about 325 ml or 8 percent of the 4.1 liter reactor volume.

Intermittent withdrawal has been found to be an effective tool for reducing classification in systems of a difficult nature (u_t - free settling velocity $> 3 \text{ cm s}^{-1}$) (1). Although this system is classified as an easy problem ($u_t < .5 \text{ cm s}^{-1}$) with maximum calculated values of u_t equal to $.075 \text{ cm s}^{-1}$, intermittent withdrawal was used to satisfy prejudices built up over the years. One unfortunate facet of intermittent withdrawal is that it imposes a cycling residence time on the tank, accentuating any tendency for instability in the crystal size distribution.

Aeschback (1) developed a crystallizer design that, although not used in this investigation, might insure complete mixing in unbaffled operation. The bottom is convoluted to follow flow streamlines and the impeller blades are reversed so center flow is upward allowing higher stirring rates without vortexing.

Previous investigators reported that steady state in a (MSMPR) crystallizer is reached after from 8 to 15 residence times (2, 4, 21). In this investigation, sampling to determine crystal size distributions and reactant concentrations was commenced ten residence times after startup.



Samples for analysis were removed from the crystallizer with a bail and beaker to avoid any inaccuracy that might arise due to nonideal mixing of the feed streams at the surface. Crystal size distributions (CSD) were determined on a size range from 8 to 25 microns, using a Coulter counter. Due to the rather primitive nature of the counter a separate analysis had to be made for each point on the crystal size distribution curve. Two points were obtained from a single sample, within 30 seconds of its removal from the crystallizer. Points were taken in pairs starting with the lowest size countable and terminating when the count fell below 15. Each count or point consisted of all particles in a 2 ml sample exhibiting an equivalent diameter greater than a lower threshold and less than an upper threshold. The raw data was fit, by least squares, using the model $[n = n^0 \exp(-L/G\tau)]$, to determine the growth rate G and the nuclei density n^0 . The computer program used for this fit can be found in Appendix A.

Analysis of reactant concentrations started with the bail-beaker system. About 150 ml of slurry was then filtered using fine filter paper in a buchner funnel. Hydroxide concentrations were determined by titrations of a 50 ml sample against 0.10 normal hydrochloric acid. A pH meter was used to determine the end points for

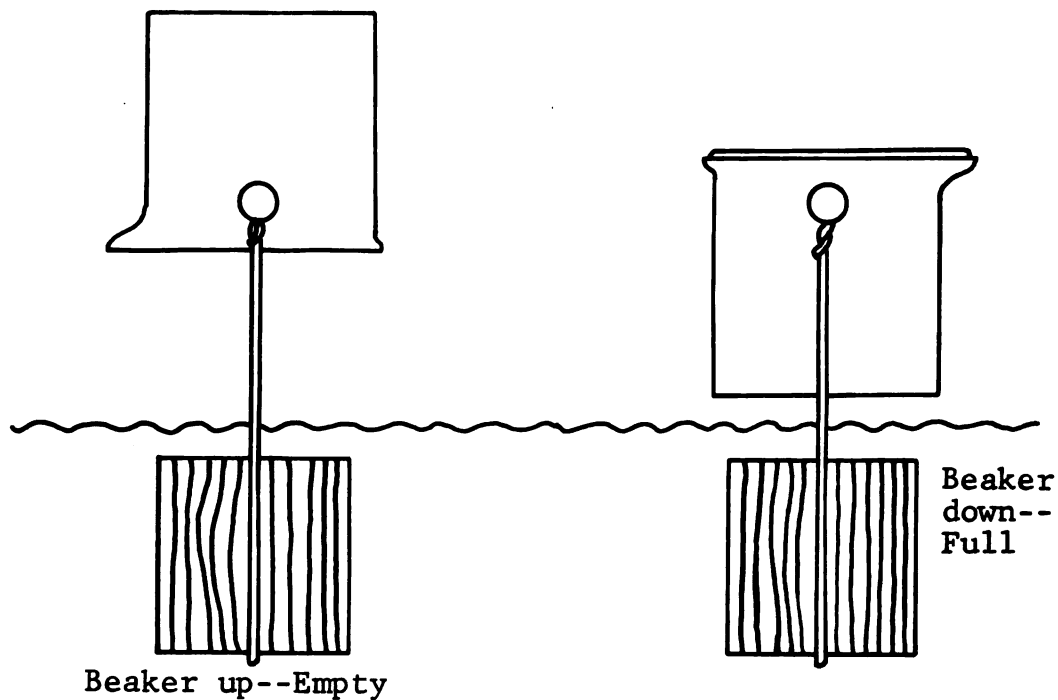


Figure 4.--Bail and beaker sampler.

total and phenolphthaline alkalinities. The iterative technique used to back hydroxide concentrations out of alkalinity measurements, its assumptions and defense, can be found in Appendix B. The same sample was then titrated against EDTA (ethylene diamine tetra acetic acid), to determine magnesium as described by Diehl (2). By lowering the pH to 4.9 in the first titration, the problem of an indistinct EDTA endpoint described by Schierholz and encountered in this work was avoided. The indistinct nature of the EDTA endpoint for a fresh

sample whose pH hadn't first been lowered to 4.9 might be attributed to some kind of a prenucleation quasi-stable association between hydroxide ions and magnesium ions. Alternative methods to determine reactant concentrations were considered, such as direct pH measurement of OH concentration, specific ion electrodes for the magnesium concentration, and conductivity measurements coupled with material balances for both concentrations. All were discarded for inaccuracy, lack of funds or lack of laboratory time for calibration. See Appendix B for a discussion of methods of hydroxide and magnesium concentration determination.

When the operator felt steady state had been reached the hydroxide reservoir was sampled and titrated to determine feed hydroxide concentration. This was necessary because the feed solution was never at equilibrium with the carbon dioxide in the air. CO₂ from the air continually dissolved in the feed, converted to carbonate and used two hydroxides in the process.



At the pH (11-11.5) where the experiments took place the driving force for this reaction was large, resulting in substantial hydroxide concentration drops overnight (on the order of 2×10^{-4} eq/l).

Temperature controllers ^a	2 Haake Model E52
Pumps feeding constant head tanks ^b	2 Eastern Industries Pump Model D-11
Filters ^c	2 Filterite Model LM010B
Filter liners ^c	6 Five Micron, Filterite Wrapped String -C5A10S
Feed pump drive ^d	1 Gill Electric Motor, Type C3/SYNCH with GEAR REDUCER
Feed pumps	2 Cole Parmer Master Flex Model 7017
Mercury switch for level control ^e	1 Mercoild Corp. Switch Model 9-51H
Stirrer drive ^f	1 Lightnin Mixer Model E
Withdrawal pump ^b	1 Eastern Rotary Pump Model VT-5
Particle counter ^g	1 Coulter Counter Model B
Filter paper	No. 42 Whatman
pH Meter	1 Corning Model 10
Air conditioner	1 12,000 BTU Comfort-Aire

Figure 5.--Equipment list and manufacturers.

^aHaake Inc.
P.O. Box 610
244 Saddle River Road
Saddle Brook, N.J. 07662

^bEastern Eng.
New Haven, Conn.

^cFilterite Corp.
Timonium, Maryland 21093

^dGill Electric
Brighton, England

^eMercoild Corp.
Chicago 41, Ill.

^fMixing Equipment Co.
Rochester, New York

^gCoulter Electronics
580 W. 20th St.
Hialeah, Florida

Between ten residence times and the end of the run, a sample of solution was filtered through a .46 micron filter and the crystals stored over Dryrite in a desiccator for later viewing under a scanning electron microscope. The electron microscope investigation was somewhat of a fishing trip; however, proper interpretation could lead to better understanding of crystallization. Photomicrographs were also taken of crystal samples from the Lansing lime-soda water treatment plant for qualitative comparison.

RESULTS

Data available for the analysis of each run consisted of the following:

- 4 to 8 sets of numbers vs. characteristic length data (crystal size distributions).
- Feed and crystallizer concentrations for Mg, OH, CO₃, HCO₃, Cl and Na.
- Feed rates and reactor volume.

The feed rates and reactor volume give residence times. When coupled with feed and crystallizer concentrations in a material balance, rate of make (eq/min) and suspension density (gm/l) can be calculated. If the crystal size distributions for each run fit the model, as they did (see Figure 6 for a representative plot), the CSD data can be reduced to growth and nuclei density versus time plots. The third moment of the CSD also gives a suspension density (22). All of these values and plots were calculated, and plotted in Appendix C. The growth and nucleation rates were averaged for each run, primarily to smooth out oscillations in the nucleation values. Results for the nine runs are tabulated in Tables 1 and 2.

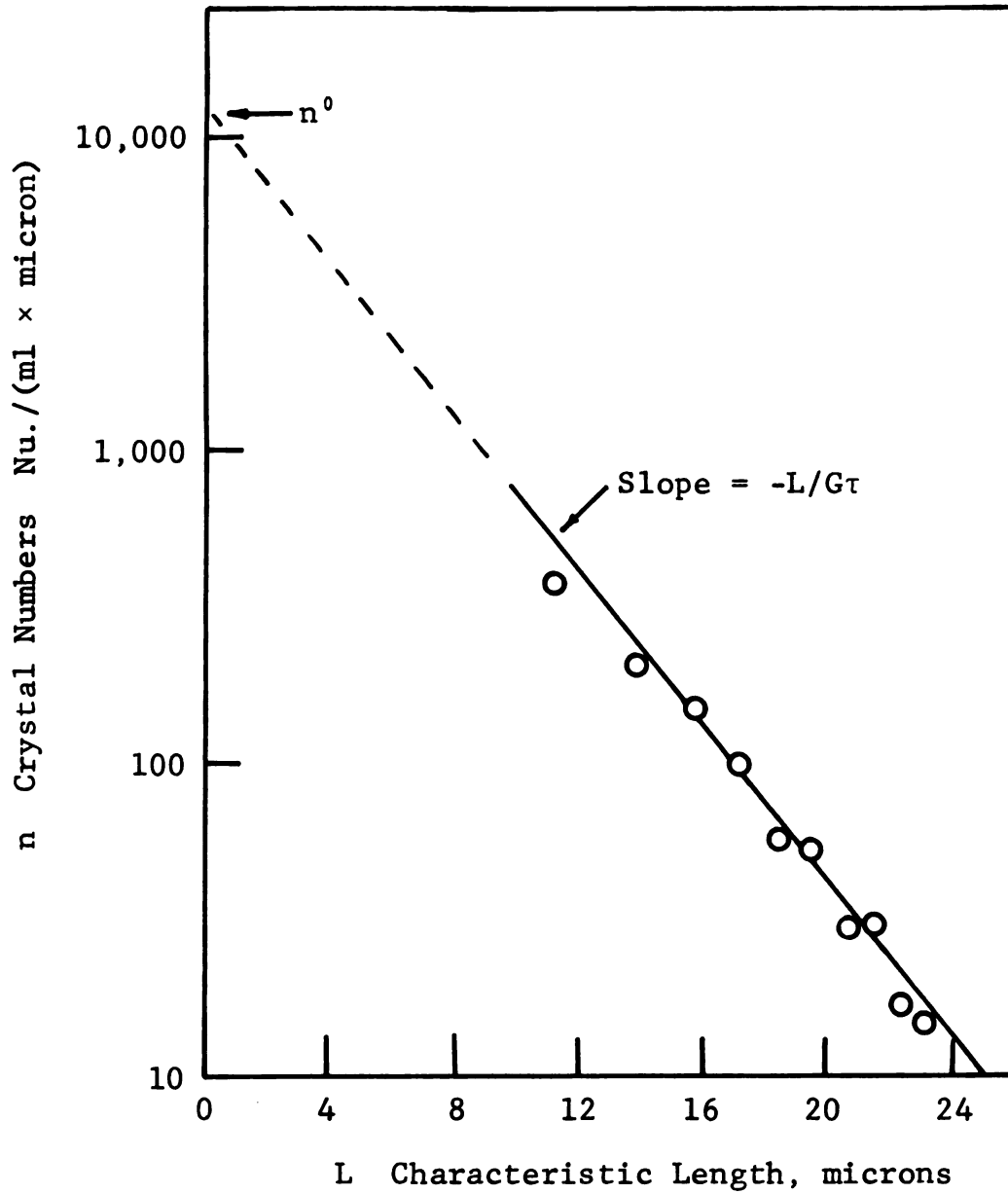


Figure 6.--Typical crystal size distribution.
Run 5-24, Series 13:20.

TABLE 1.--Results from material balance.

Date	Residence Time minutes	C_{OH} eq/l $\times 10^4$	C_{Mg} eq/l $\times 10^4$	Rate of Make		Make Ratio OH/Mg	Suspension Density gm/l
				Hydroxide ⁴ eq/min $\times 10^4$	Magnesium ⁴ eq/min $\times 10^4$		
5-10	12.40	12.37	6.51	2.69	2.10	1.28	.022
5-13	7.72	14.44	7.72	2.69	2.70	1.00	.015
5-15	20.54	12.84	5.62	1.69	1.51	1.12	.023
5-22	12.98	16.18	4.87	2.25	1.67	1.35	.018
5-24	12.86	19.22	4.14	2.19	1.44	1.52	.016
5-27	13.01	30.28	1.91	2.81	1.48	1.89	.020
6- 3	20.32	31.47	1.67	1.79	1.01	1.77	.020
6- 5	8.07	20.18	4.92	2.73	1.84	1.49	.013
6-8	8.07	27.15	2.92	3.62	2.07	1.75	.016

TABLE 2.--Results from crystal size distribution.

Date	Residence Time minutes	C_{OH} eq/1x10 ⁴	C_{Mg} eq/1x10 ⁴	Growth Rate micron/min	Nucleation Rate nu/min/ml	Suspension Density gm/l
5-10	12.40	12.28	6.58	.345	1750	.013
5-13	7.72	14.64	7.37	.405	5360	.009
5-15	20.54	13.95	5.53	.241	1240	.023
5-22	12.98	16.19	4.87	.315	1770	.012
5-24	12.86	19.22	4.14	.265	3030	.011
5-27	13.01	30.28	1.91	.227	4050	.010
6- 3	20.32	31.47	1.67	.168	2080	.013
6- 5	8.07	20.18	4.92	.350	5820	.008
6- 8	8.07	26.75	2.86	.305	5070	.005

Figures 7 through 20 are photomicrographs taken with a scanning electron microscope. Figures 7 through 15 are from the laboratory runs. Figures 7, 8 and 9 show the flake and plate crystals found in short residence time samples, while Figures 10 through 15 show the variety of crystals found at longer residence times. Figures 16 through 20 make up a progression of the kind of crystals found in samples from the Lansing water softening plant, starting with Figures 16 and 17 from after the rapid mix basin, and progressing with Figures 18, 19 and 20 through flocculation basins (see Figure 1, slow mix). The magnification in each picture is given. Relative sizes can be determined by remembering that for 10,000X magnification, one centimeter in the photograph equals one micron in actual crystal dimensions.

Figure 7.--Solid crystal with a clump of small flake aggregates, Run 5-24 (1000X).

Figure 8.--Detail of Figure 7, edge shot of star aggregate, center and "nuclei" lower right, Run 5-24 (10,000X).

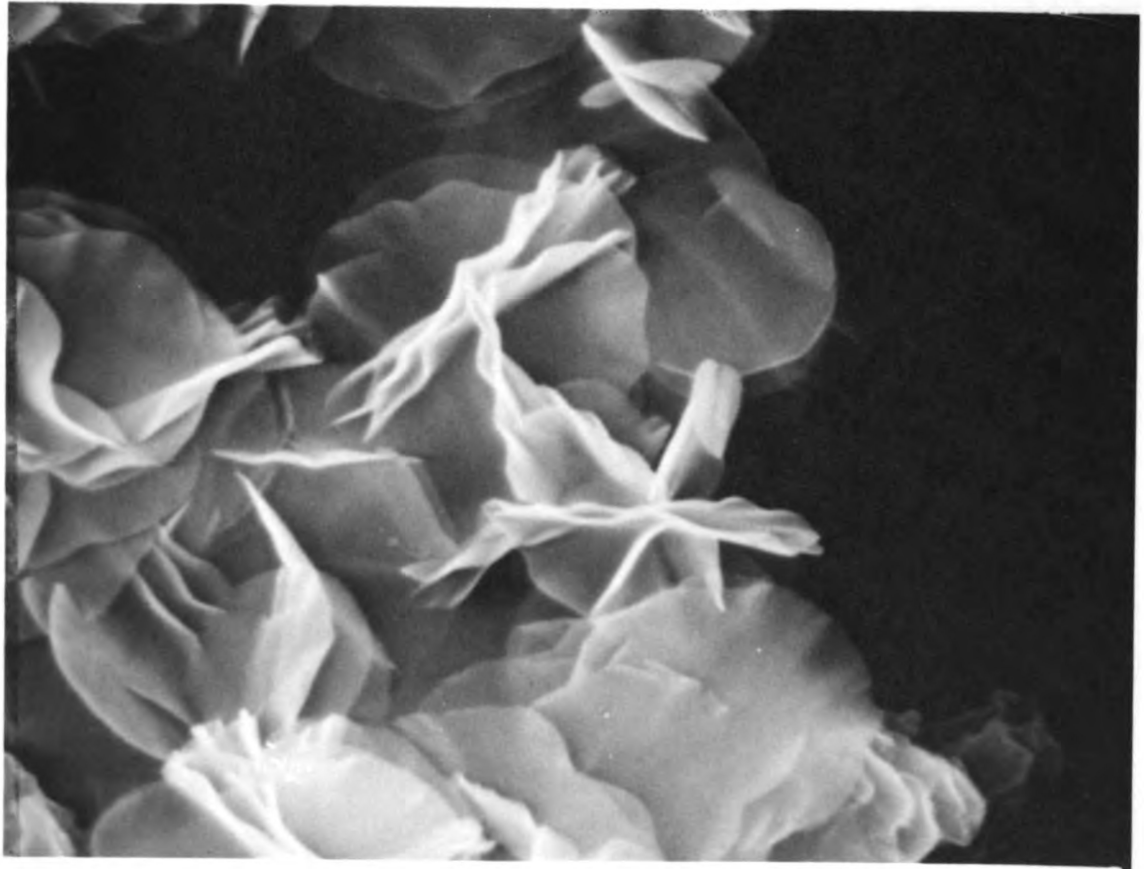
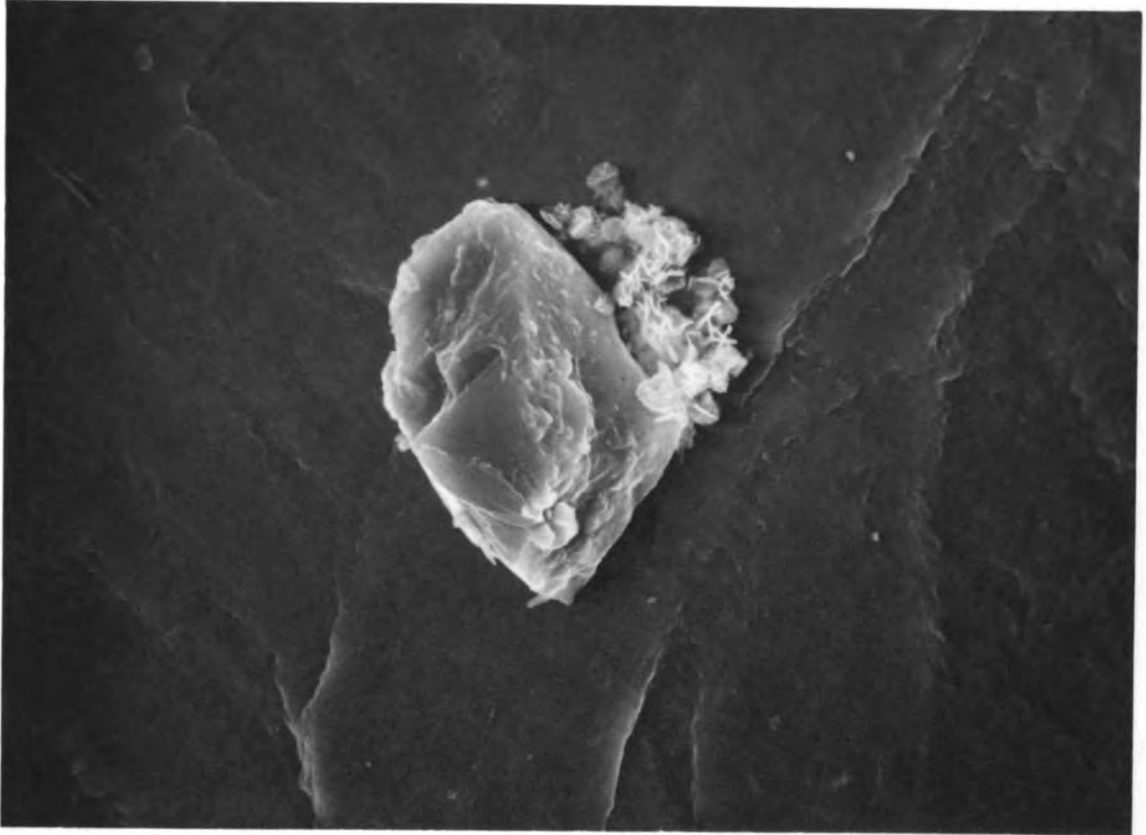


Figure 9.--Crystal flakes and aggregates, thin edge lower right center, Run 6-8 (10,000X).

Figure 10.--Unusual "sponge" crystal formed at 20 minute residence time, Run 6-3 (2000X).

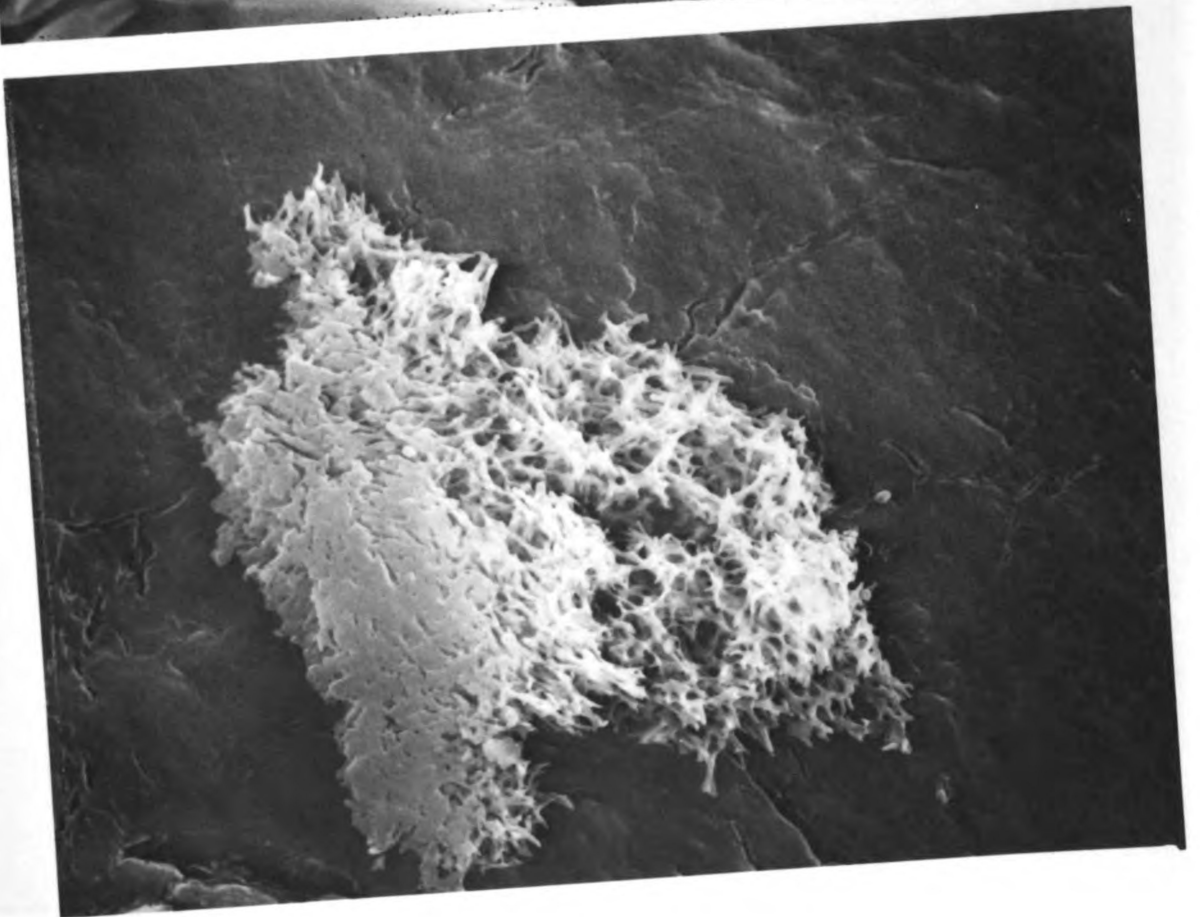
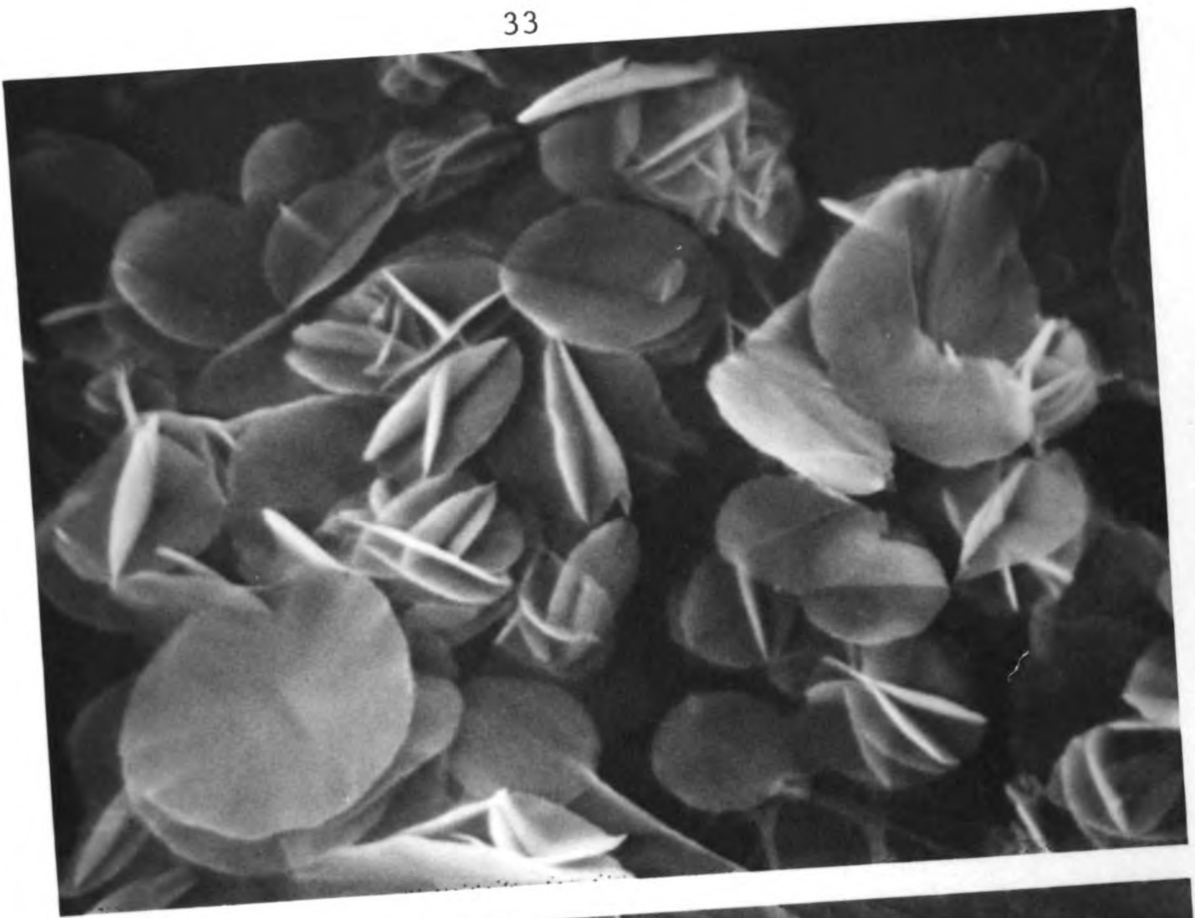


Figure 11.--Solid crystal, fairly common at longer residence times, Run 6-3 (2000X).

Figure 12.--Unusual hollow "needle" crystal, Run 6-3 (500X).

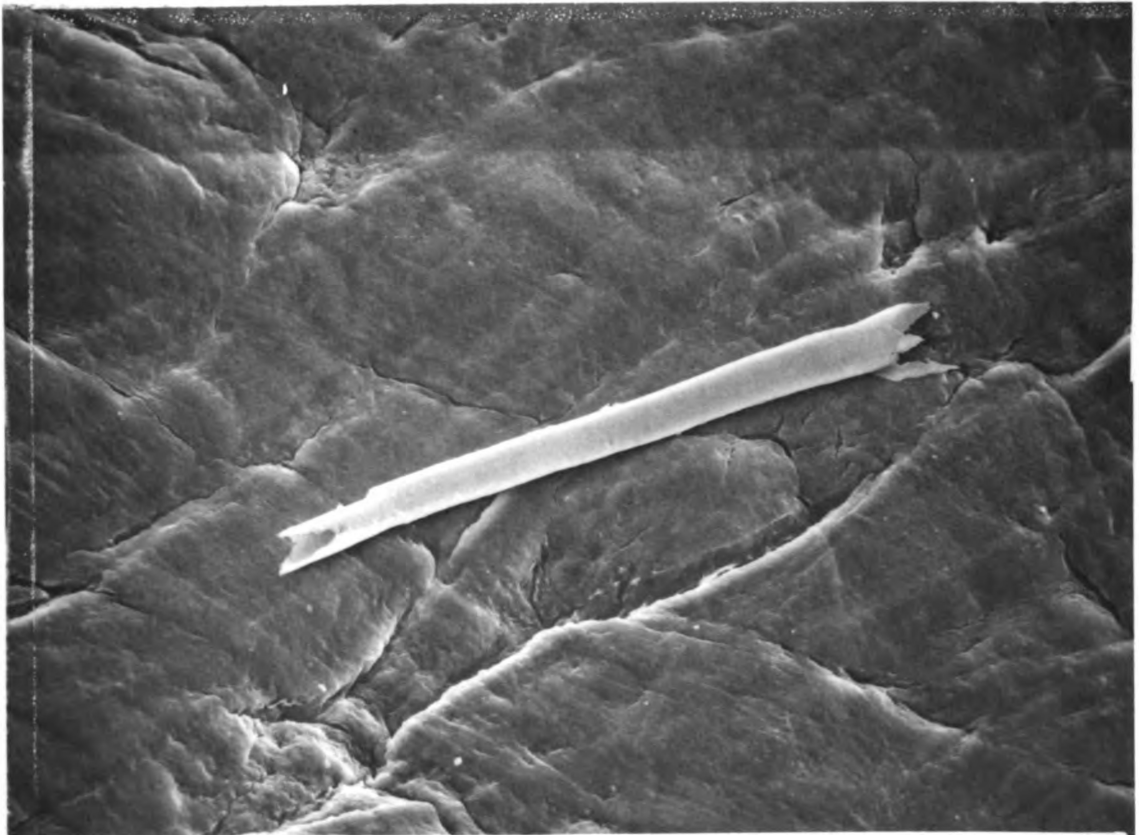
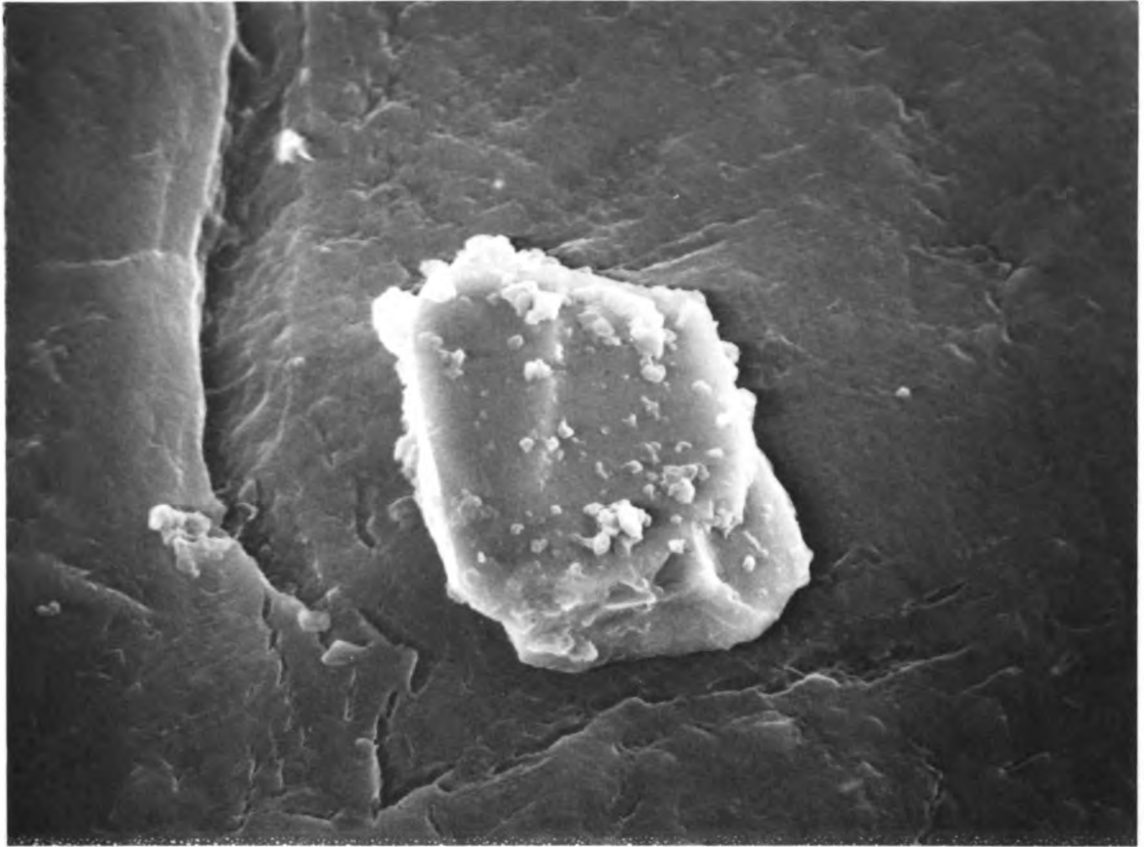


Figure 13.--Detail of Figure 12, point of needle crystal, Run 6-3 (2000X).

Figure 14.--Large solid crystal, plate-like appearance, Run 5-15 (1000X).

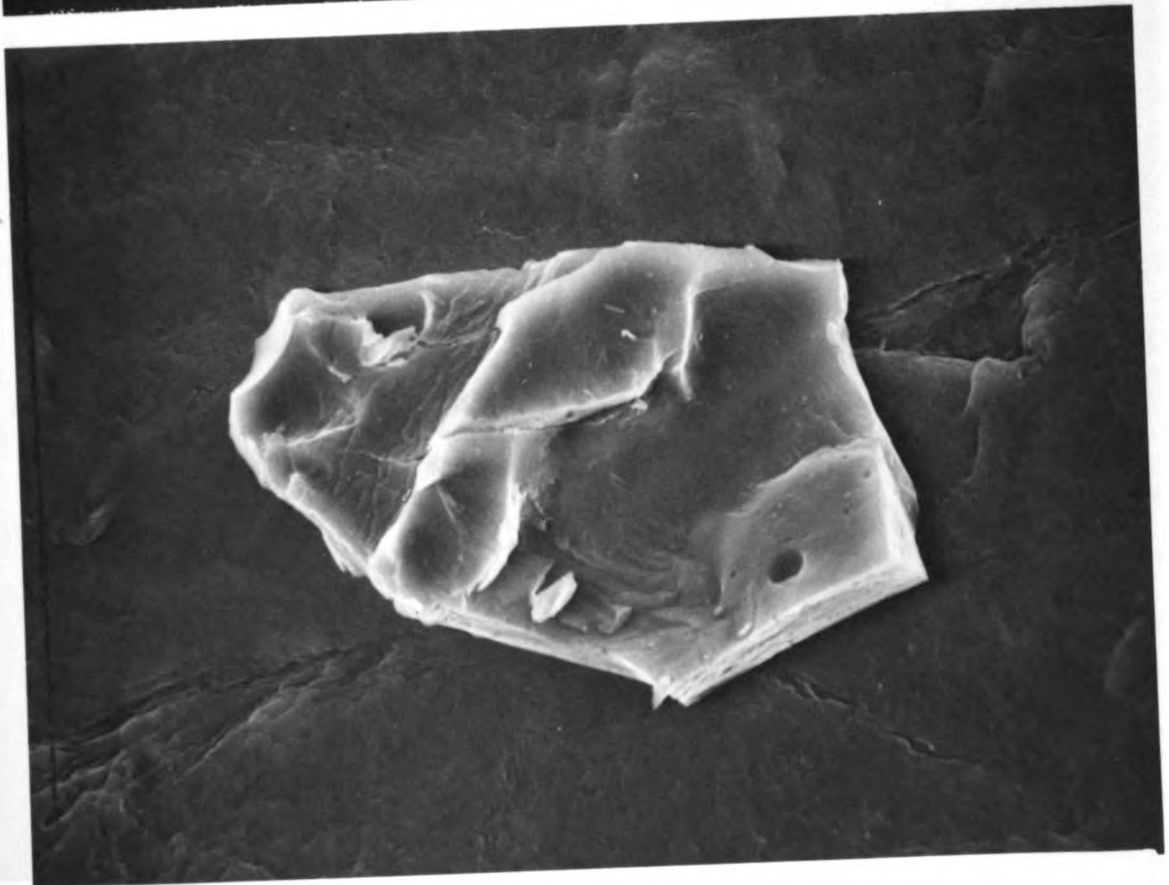
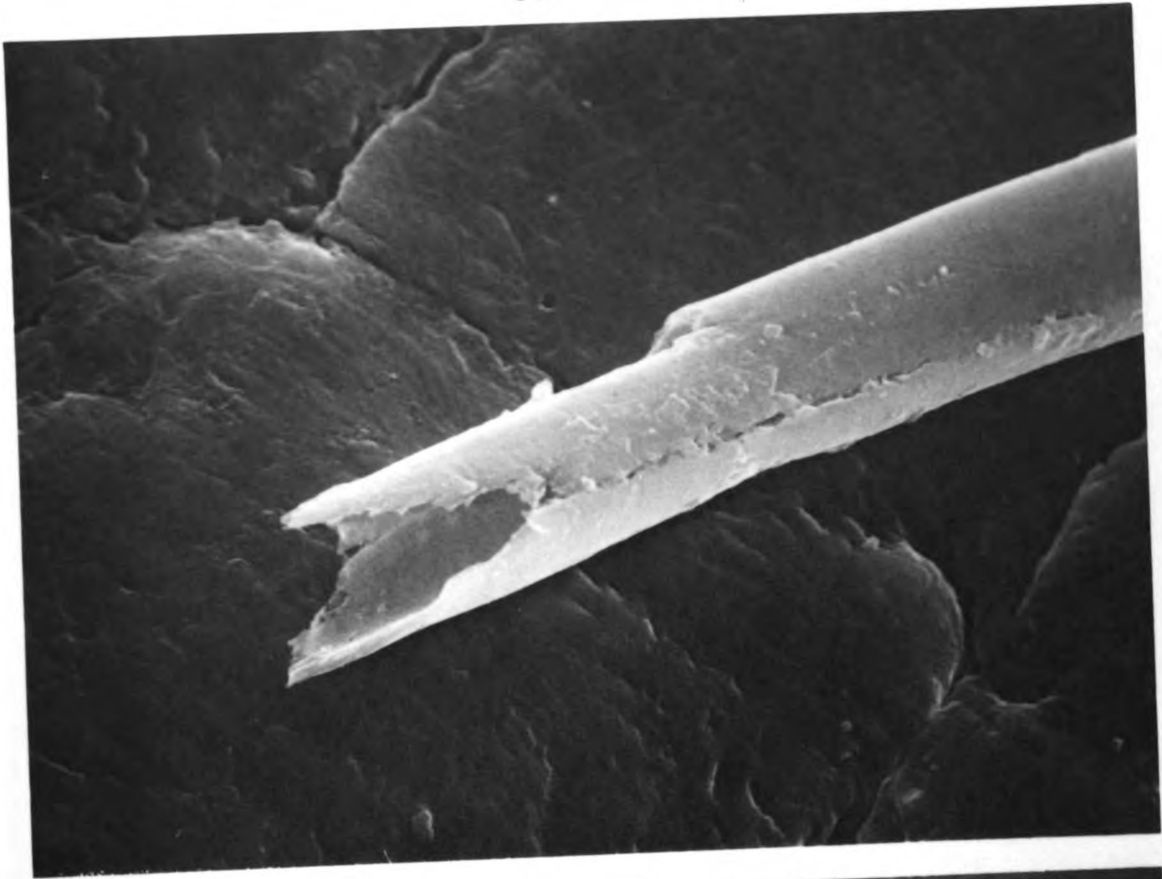


Figure 15.--Large clump of flake aggregates, most commonly seen crystals in the laboratory samples, predominant at shorter residence times, Run 5-15 (2000X).

Figure 16.--Agglomerate taken after the rapid mix area of the Lansing drinking water treatment plant, representative formation (5000X).

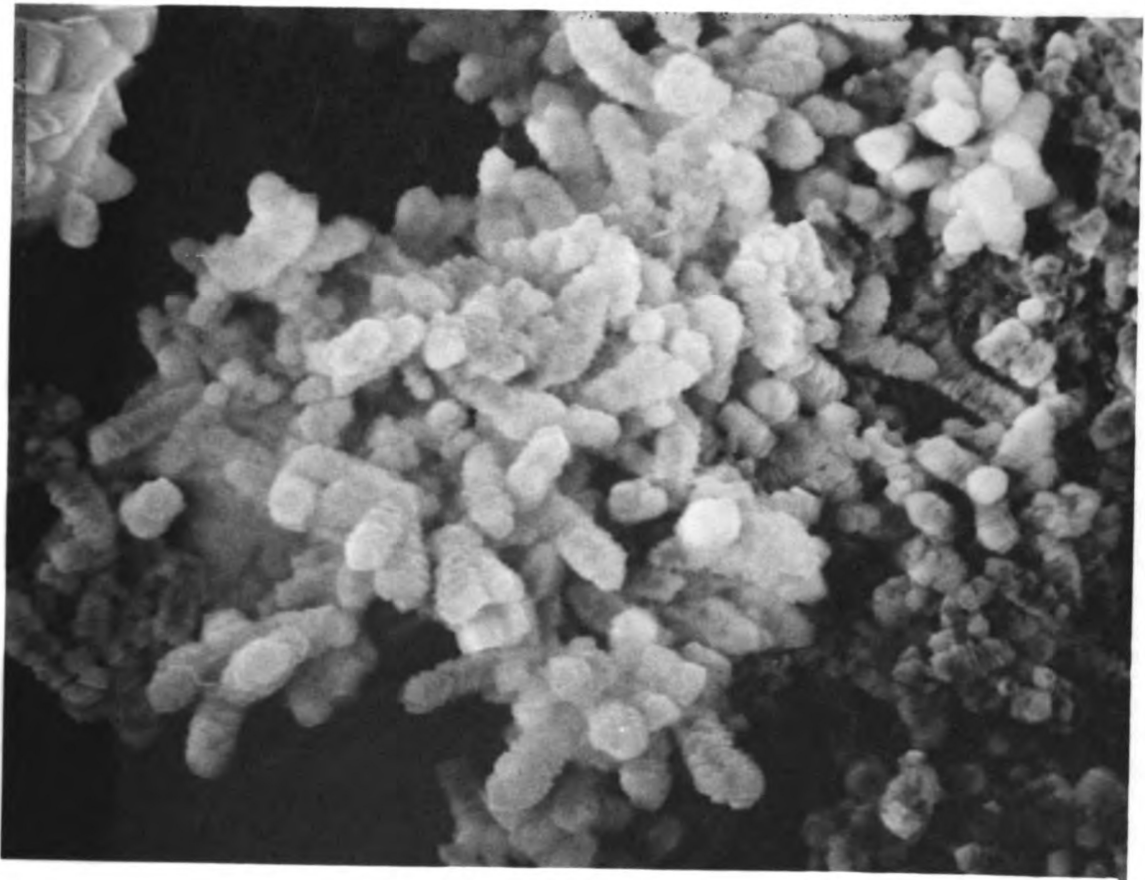
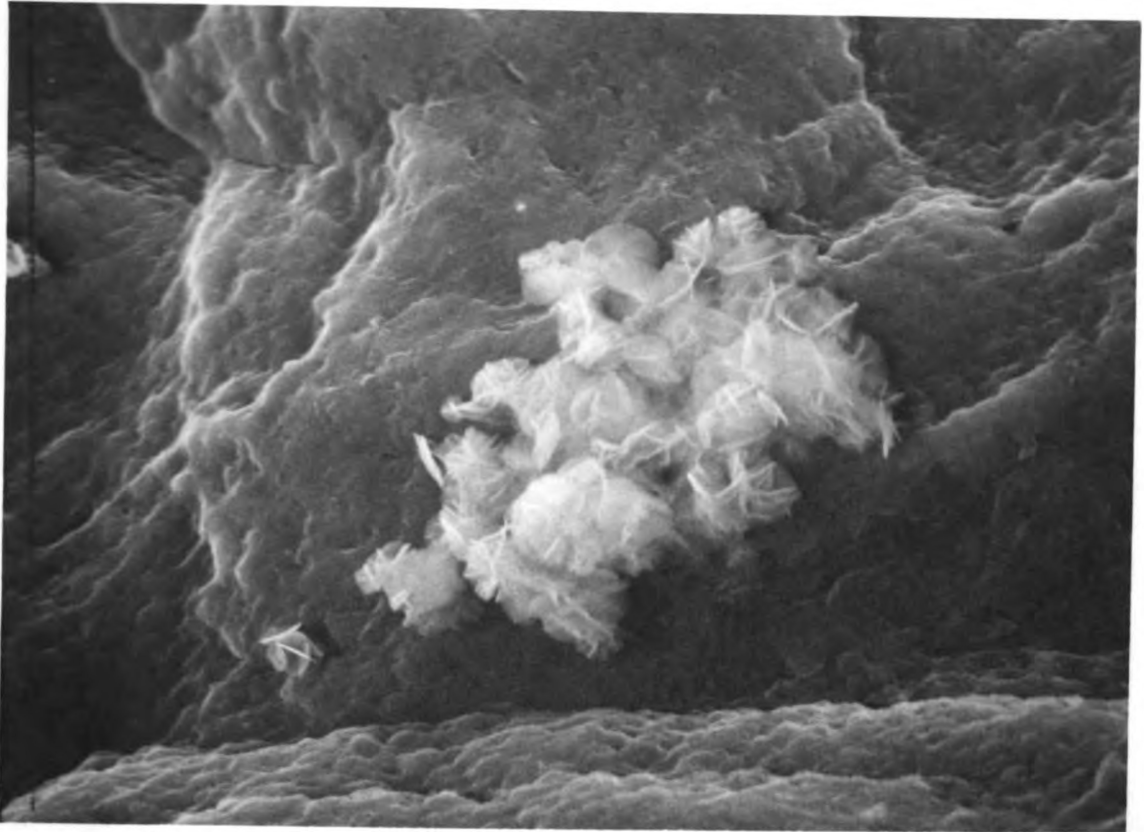


Figure 17.--Layered finger, representative of sample taken after the rapid mix. The agglomerate melted under the electron beam suggesting that it is "soft" (10,000X).

Figure 18.--Representative agglomerates from the first flocculation basin. The layers in the fingers are filling in (5000X).

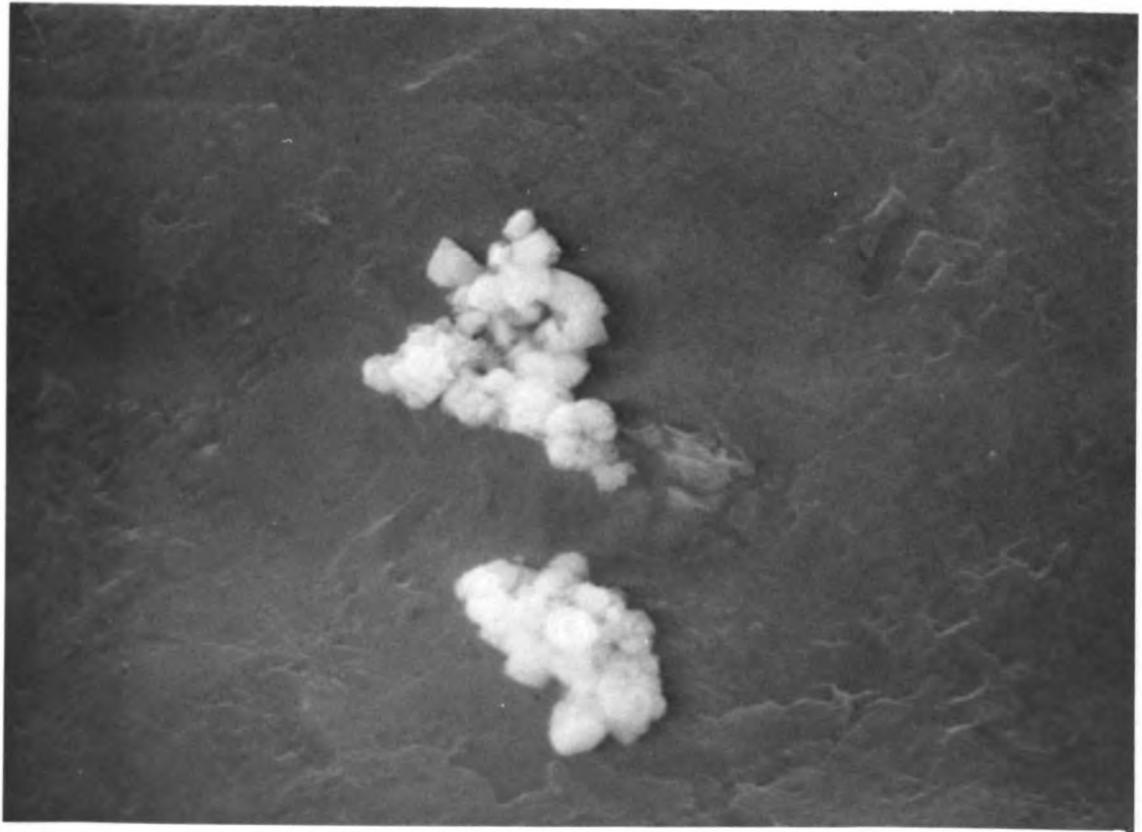
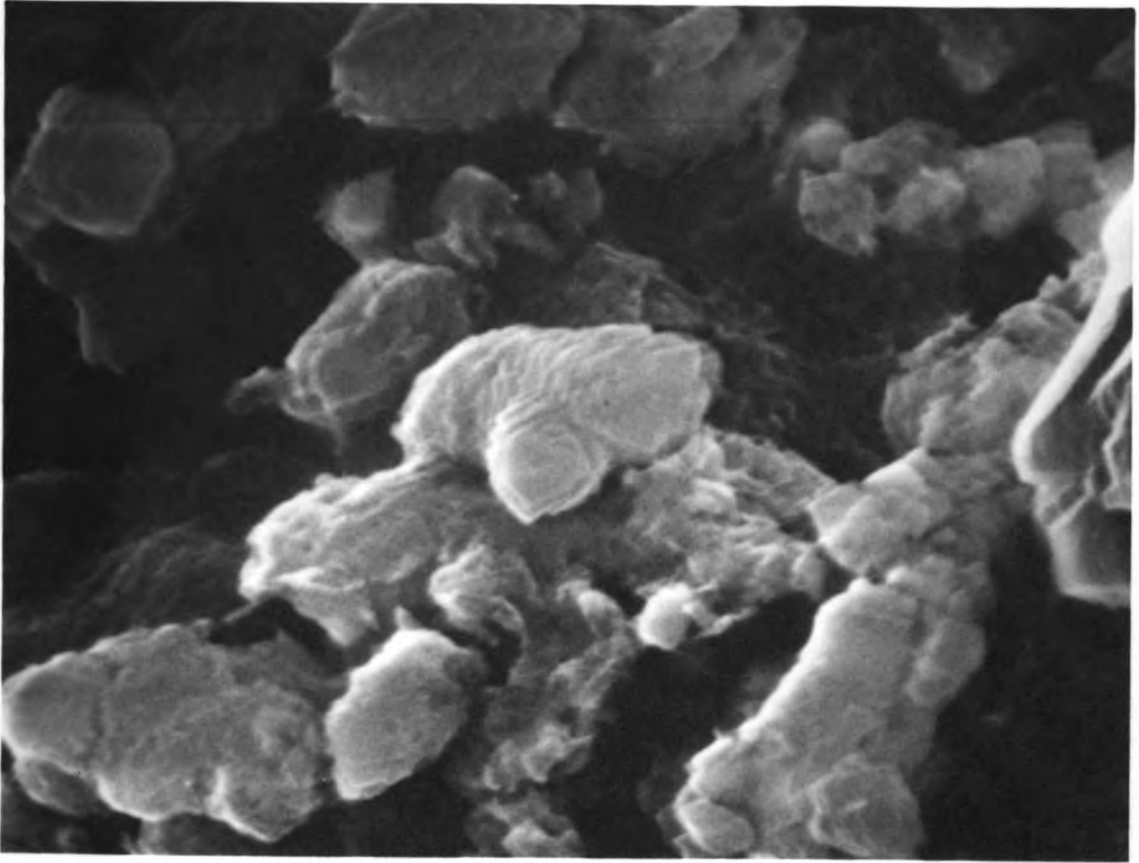
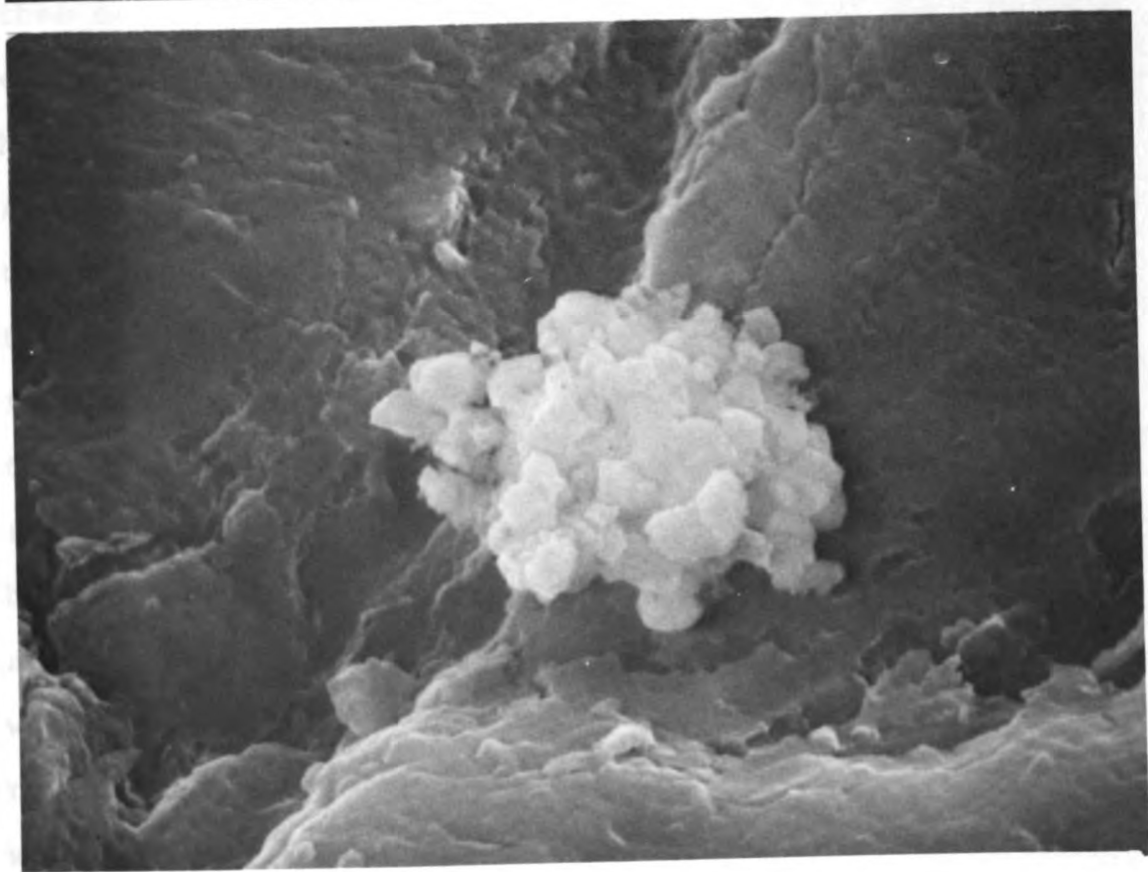
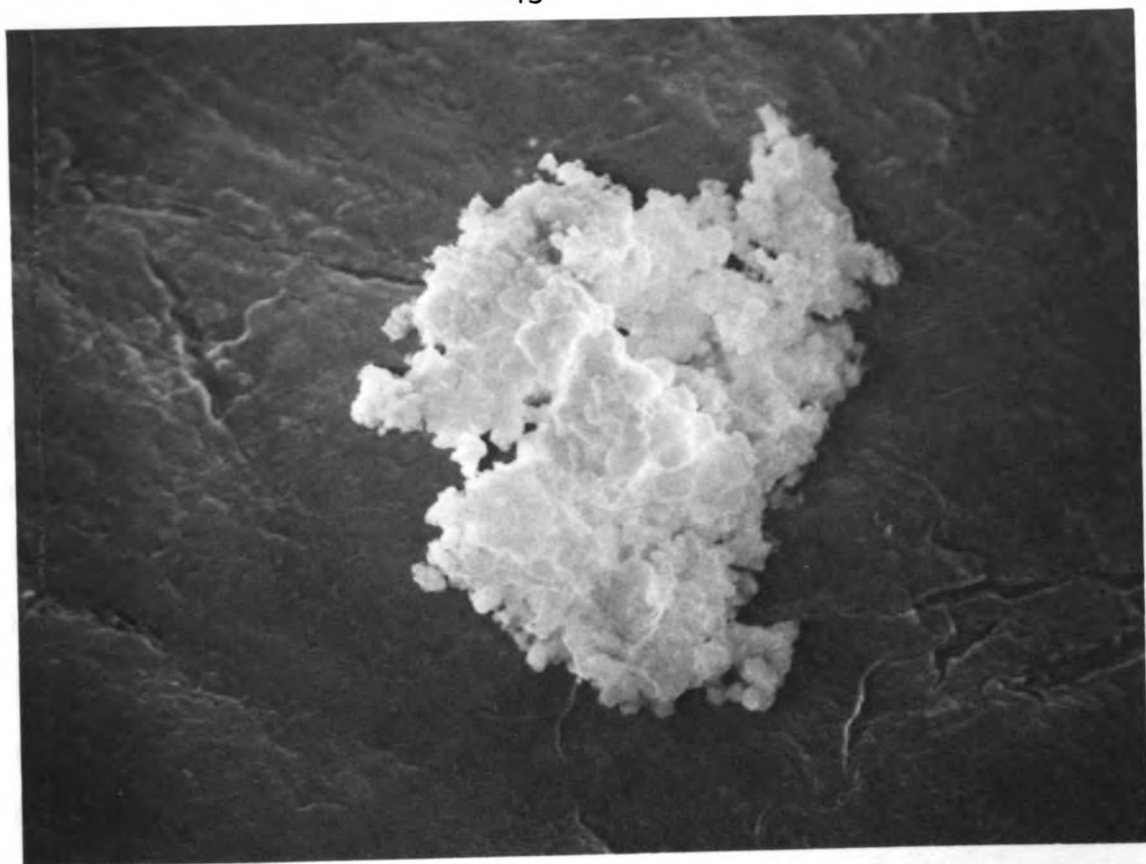


Figure 19.--Representative agglomerate from the third flocculation basin. The spaces between the fingers are filling in (2000X).

Figure 20.--Representative agglomerate from the fifth and last flocculation basin. The particle appears more solid than those from earlier flocculation basins but is not very big. Settling velocity is calculated at 14 centimeters per hour (5000X).



DISCUSSION

The material balance data raises some serious questions about the accuracy of the analytical techniques. Accurate analysis should certainly give equal rates of make for hydroxide and magnesium but the data shows ratios of hydroxide over magnesium rates of make ranging from the expected one, one to two. Reservoir concentrations, feed rates, reactor volume, and round-off determinations all have room for error but none of them can justify errors of this magnitude. Crystallizer concentration determination must be the culprit. Perhaps the picture of a complete filtration separation is at fault: hydrated, neutral, dry $\text{Mg}(\text{OH})_2$ crystals on the filter paper and supersaturated, clear solution in the filter flask. Deviation from the ideal could come in two ways. Small crystals could have passed through the filter or some of the solution could have stayed on the filter paper with the crystals. The first possibility, crystals in the supernatant, would result in a lower rate of make, but it is hard to envision why it would skew the calculated ratio of hydroxide to magnesium in the crystalline mass. Film theory coupled with a bit of supernatant staying on the filtered

crystals may be the cause. The film adjacent to the crystals may have a higher ratio of one reactant over the other reactant than the bulk solution. Since the ratios of rate of make of hydroxide over magnesium were equal to or greater than one, the film may have been composed of sodium hydroxide. The concentrations follow trends compatible with the film theory wet crystals postulate. Higher hydroxide concentrations favor higher ratios and lower hydroxide concentrations favor lower ratios. If this is the case, what does it mean? Wet crystals mean that both the hydroxide and the magnesium crystallizer concentrations are actually bulk concentrations, if the whole boundary layer stayed with the crystals. That is fine for driving force determinations but crystals plus boundary layer are no way to measure suspension density.

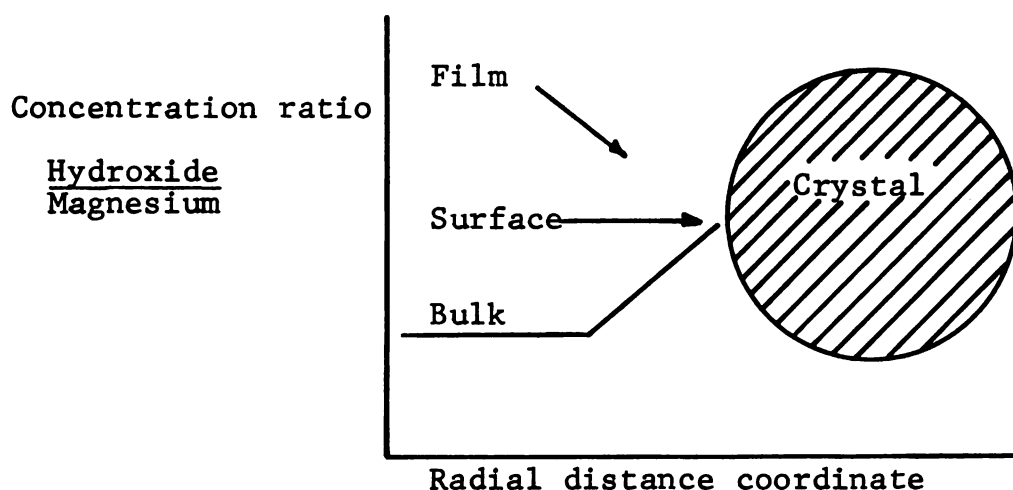


Figure 21.--Film theory for magnesium hydroxide growth.

Suspension density (grams of crystals per liter of solution) was calculated by two techniques. Rate of make for magnesium (R_{Mg}) and hydroxide (R_{OH}) was calculated from the material balance and converted to suspension density (M_{T1}).

$$M_{T1} = (R_{Mg} 12.16 + R_{OH} 16) \tau / V$$

The crystal size distribution also gives suspension density when it fits the model (22).

$$n = n^0 \exp(-L/G\tau), B^0 = Gn^0$$

$$M_{T2} = 6\rho k_v B^0 (G\tau)^4 / G$$

The CSD data nicely fit the model so M_{T2} values were calculated (see Table 2). The anticipated correlation of equal suspension density by the two methods was absent. Ratios of M_{T2} over M_{T1} ranged around .6. To rationalize these results it is necessary to once again cite film theory, with a pinch of crystal lattice induction. It is well known that a crystal seed induces crystallization. In solution the crystals could be surrounded by a layer of fluid crystalline NaOH, MgOH and $Mg(OH)^2$ which when filtered would stay with the crystals and skew the suspension density calculations. Such a fluid crystal would conduct electricity as an electrolyte so that when a crystal plus film was

measured by a Coulter counter only the solid non-conducting crystal would be measured. Another possible explanation for the divergent suspension density calculations is raised by the narrowness of the analyzed portion of the CSD. Classified withdrawal could leave an unmeasured but significant number of large crystals in solution, having a large enough area for deposition to change rate of make and thus the suspension density. This situation would have shown itself by continual plugging of the 140 micron aperture on the Coulter counter. Although plugging did occur, it was not so frequent as to make this a highly probable situation.

A third possible explanation for inaccurate suspension density again based on the narrowness of the CSD curve is raised by the electron microscope studies.

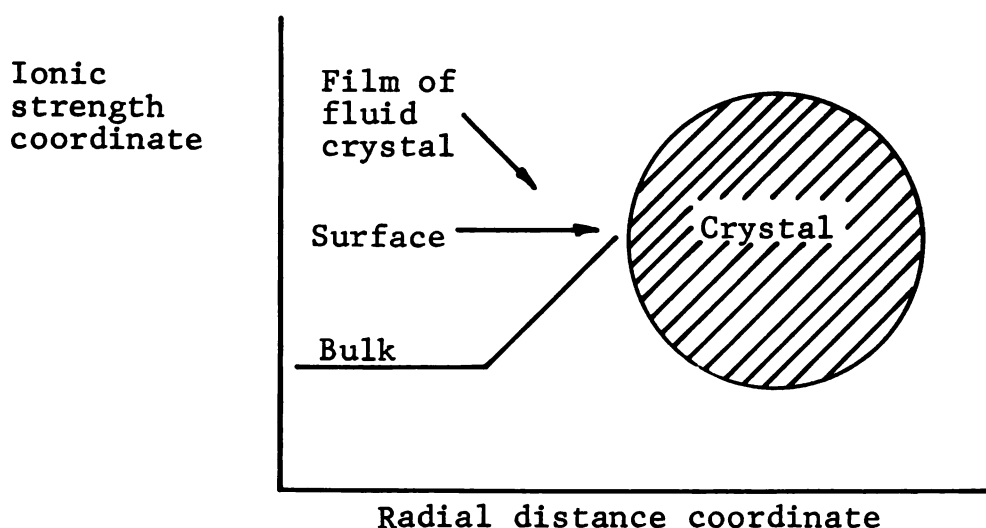


Figure 22.--Film theory for induction of high ionic strength near a growing crystal.

A tremendous number of clumps of small flakes like those in Figures 8, 9 and 15 were seen. The width of the flakes was normally less than 3 microns while some individual flakes were only 50 angstroms thick, so they might not be counted accurately by the Coulter counter. If their numbers deviated from the model on the high side this, too, could account for erroneous suspension densities. This explanation is suspect because of the immense numbers necessary to affect the rate of make. It is interesting to note that on a day the make ratio was close to one (5-15), the suspension densities by both methods correlated closely. This run had a long residence time (20 min) and the lowest recorded nucleation rate. Schierholz (25), who also experienced divergent suspension densities, had good correlation at his highest residence times (30 min). It may be that the slower growing crystals from the longer residence time runs exhibit less crystalline induction resulting in better correlation of suspension densities.

The crystal pictures obtained from the electron microscope certainly laid to rest thoughts about strict similarities between crystals grown in the laboratory and those found in lime-soda and industrial processes. Neither the vaterite form of calcium carbonate that Schierholz (25) found to predominate his samples nor any of the several habits of magnesium hydroxide (Figures 7

through 15) found in this study could be found in the Lansing water softening plant samples. What was found could be described as layered, uniformly amorphous aggregates (Figures 16 through 20).

Even though the crystal habit varied the crystal size distribution data nicely fit the birth-growth model, $n = n^0 \exp (-L/G\tau)$. Birth and growth rates were plotted against reactant concentrations to find a model for nucleation and growth in this system. The only plots that gave anything vaguely reminiscent of a fit are plotted in Figures 23 and 24, with a least squares fit straight line. The growth rate versus reactant concentration product plot is a good fit showing an average deviation of 8 percent. The nucleation rate versus reactant concentration product fit is not so nice; average deviation is 22 percent. Three points, 5-10, 5-13, and 6-3, cause most of the problems with deviations of 49, 53, and 45 percent, respectively. Ignoring them, the average deviation from the same straight line dips to 11 percent, a more respectable figure. The Debye Huckel limiting law (18) was applied to attempt a better fit but it was found that activity coefficients for hydroxide were .96 for all runs and for magnesium varied only from .85 to .86, so fits were not improved. Since the limiting law is based on a model of completely dissociated ions and this system is highly associated,

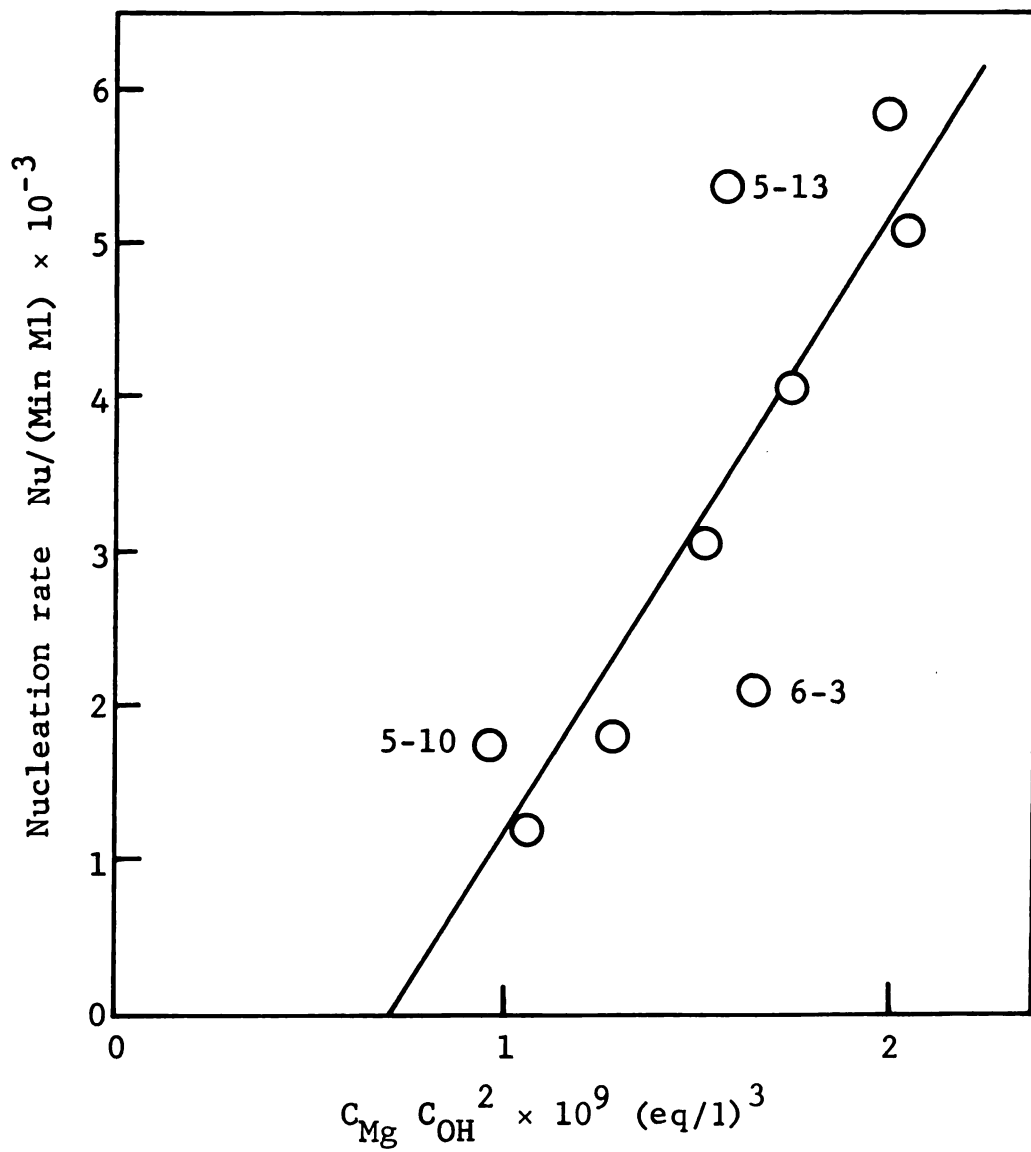


Figure 23.--Nucleation rate as a function of reactant concentrations.

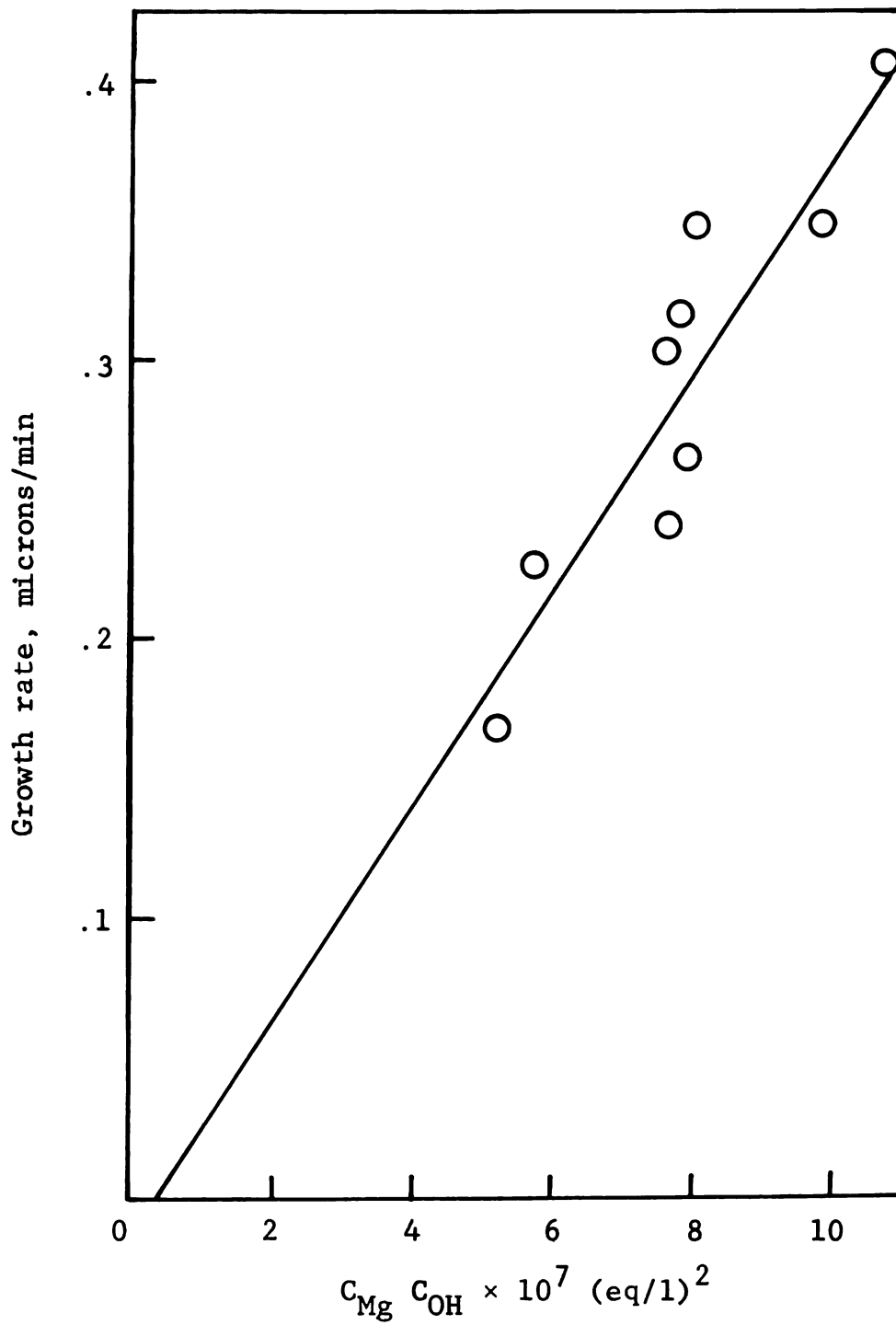


Figure 24.--Growth rate as a function of reactant concentrations.

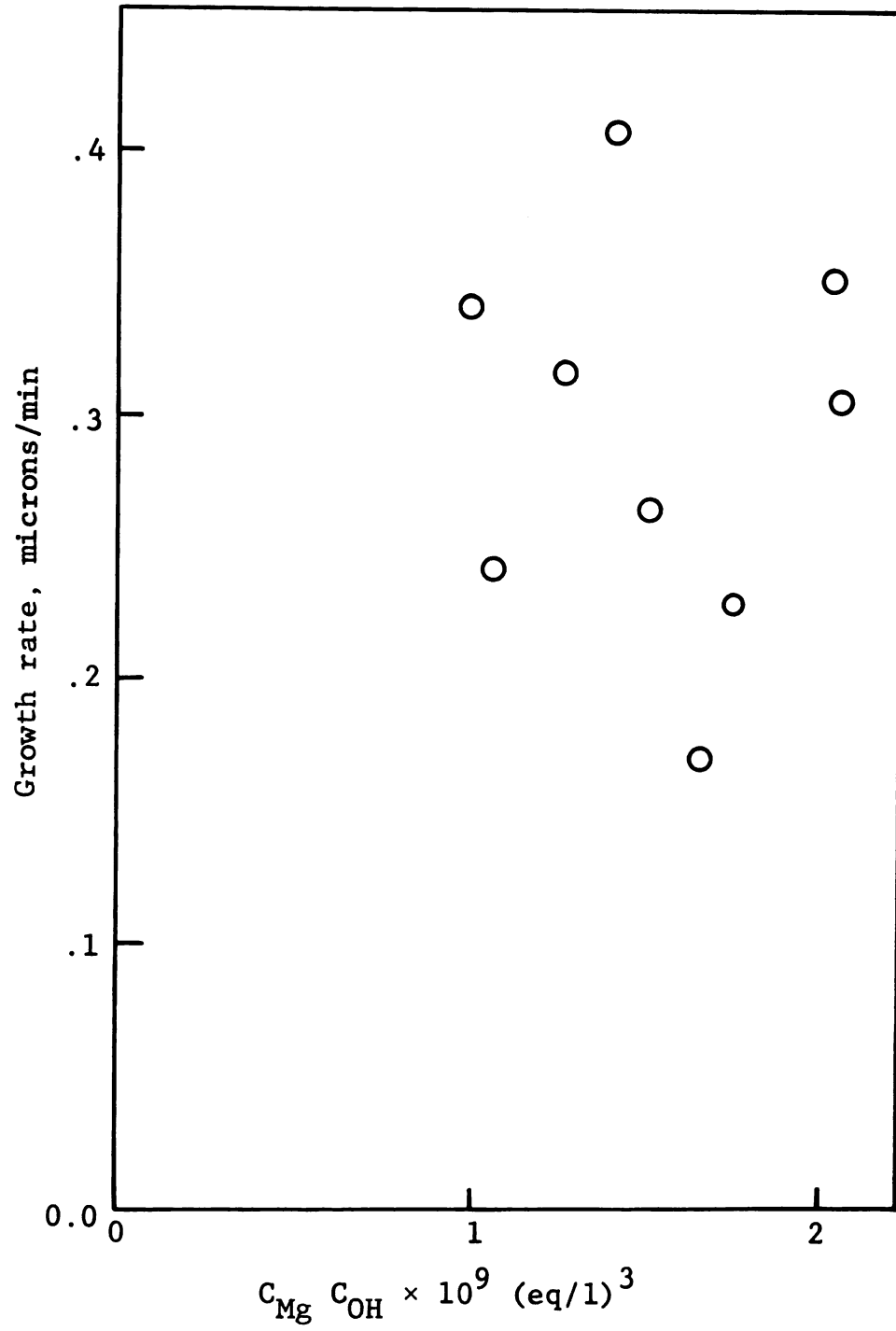


Figure 25.--Growth rate versus $C_{Mg} C_{OH}^2$.

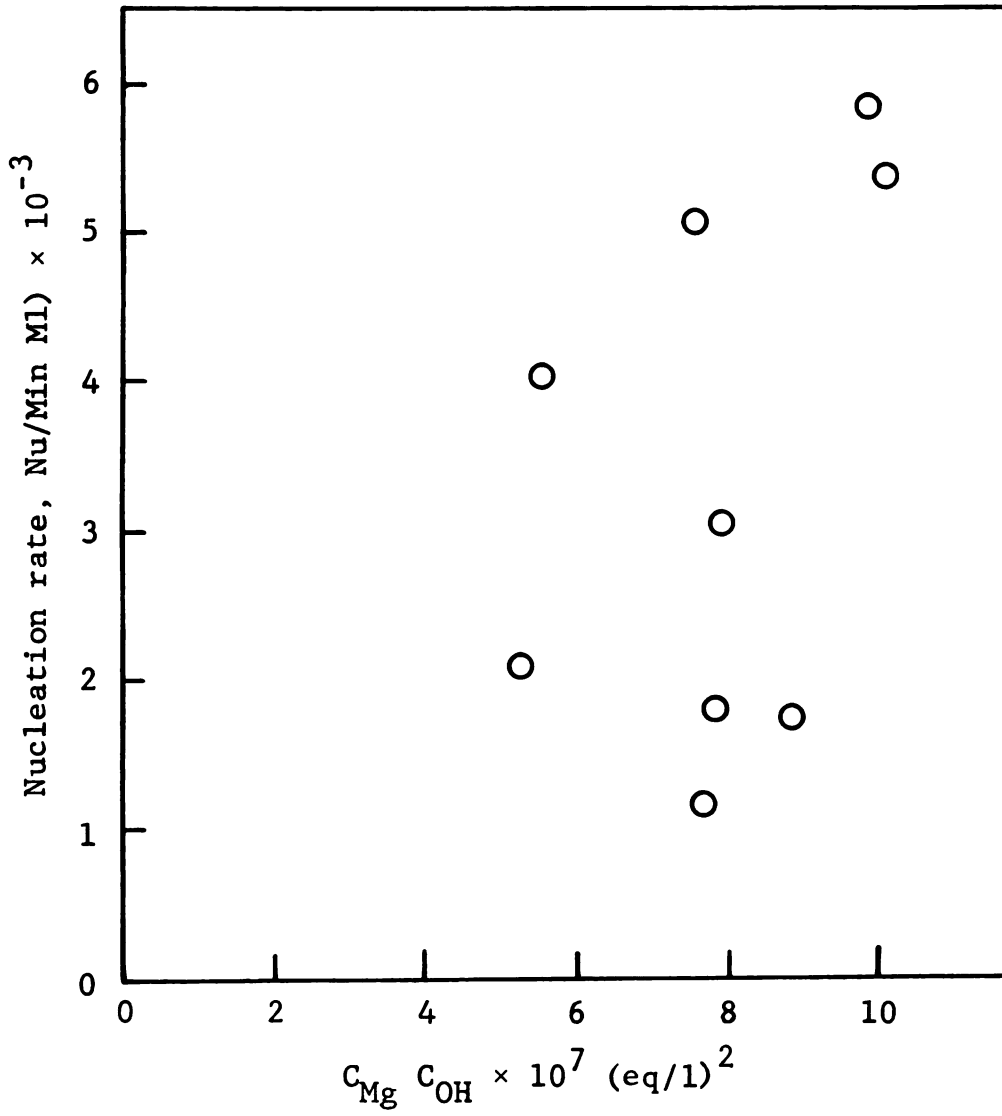


Figure 26.--Nucleation rate versus $C_{\text{Mg}} C_{\text{OH}}$.

concentration was chosen rather than activity to characterize the solutions. The fits are:

$$G = 3.83 \times 10^5 (C_{\text{OH}} \times C_{\text{Mg}} - 2.97 \times 10^{-8}) \quad (1)$$

$$B^0 = 3.95 \times 10^{12} (C_{\text{OH}}^2 \times C_{\text{Mg}} - 6.95 \times 10^{-10}) \quad (2)$$

If a new supersaturation were defined it would have to be different for growth than for nucleation, having an extra hydroxide term in the nucleation based supersaturation. If these equations were used to model the system it would be necessary to define a discontinuous slope for the birth rates so negative birth rates would be avoided.

$$B^0 = 0 \quad \text{for } C_{\text{OH}}^2 \times C_{\text{Mg}} < 6.95 \times 10^{-10} \quad (3)$$

Negative growth rates are expected in unsaturated solutions but are probably not described accurately by the model; they involve extrapolation in the extreme. Equation (2) correlates with the literature in form if not in exponential powers (see Background).

In a precipitation separation system like lime-soda water softening the object is to make large solid particles that can easily be separated by settling. This can be accomplished by minimizing nucleation so fewer small slow settling crystals are formed and maximizing growth so large crystals and solid agglomerants

are formed. If nucleation is ignored, rate of make becomes a function of particle surface area and growth rate, which is maximized by maximizing surface area and growth rate. To minimize nucleation while maximizing growth rate appears an impossible task due to the shape of the curves. The configuration of the Lansing water treatment system enlightens the analysis. The series of six backmix reactors could be roughly modeled as a plug flow reactor (with the reactants mixed at the entrance). This causes high rates of nucleation near the entrance with relatively little advantage accrued from the high growth rate near the entrance because of a general lack of crystal surface area. If the hydroxide feed were spread out along the reactor length, nucleation rates would be leveled along with hydroxide concentrations. This would also lower growth rates and consequently rate of make. Recycle of primary sludge would increase the area available for deposit and get the rate of make back up to where it should be; the resulting large crystals would settle quickly to form a sludge high in solids, as reported by the literature. A quantitative modeling of the lime-soda ash water softening system should wait until kinetics are in from a study of continuous co-precipitation of magnesium hydroxide and calcium carbonate. The electron microscope survey of Lansing's system indicates only one crystalline

form is precipitated. Since both magnesium hydroxide and calcium carbonate are being precipitated it might be a co-crystal containing both. Kinetics for its formation may be a function of all four reactants.

CONCLUSIONS

The population balance as adapted by Schierholz and Stevens (26) to dilute precipitation systems applies to the magnesium hydroxide system, because McCabe's ΔL law holds in the range of crystal sizes used in this investigation. Species concentrations can be used to describe the nucleation and growth rates. Supersaturation has to be defined separately for nucleation and growth.

$$s_g = C_{OH} \times C_{Mg} - 2.97 \times 10^{-8} \text{ (equivalents/liter)}^2$$

$$s_n = C_{OH}^2 \times C_{Mg} - 6.95 \times 10^{-10} \text{ (equivalents/liter)}^3$$

With this definition of supersaturation, Equations (1) and (2) become:

$$G^0 = K_g \times s_g \quad K_g = 3.83 \times 10^5 \text{ microns/minute (liter/eq)}^2$$

$$B^0 = K_n \times s_n \quad K_n = 3.95 \times 10^{12} \text{ crystals/(min ml) (liter/eq)}^3$$

$$B^0 = 0 \quad \text{for } K_n \times s_n \leq 0$$

The scanning electron microscope study shows that the system here modeled by population balance and

the one encountered in the Lansing water softening plant are two very different entities. There is no evidence to indicate that Equations (1) and (2), developed to describe magnesium hydroxide precipitation, can be used even in part to describe water softening because no crystals of the habits found in the crystallizer were found in the treatment plant. The fact that the crystals from the treatment plant were predominantly of a single habit raises the possibility that a future investigation of co-precipitation of $Mg(OH)_2$ and $CaCO_3$ would result in a model useful in water softening plant design. In any future study, one should check the crystal habit obtained for co-precipitation in the laboratory with that found in water treatment plants.

RECOMMENDATIONS

Lime-Soda Ash Water Softening

1. Distribute some slaked lime to the flocculation basins.
2. Slake the lime with treated water if that is not already the practice.
3. Recycle primary sludge.
4. Enlarge the rapid mix volume (see Figure 1).

Lime-Soda Ash Modeling Study

1. Consider alternative direct analysis methods for reactant concentrations.
2. Use the crystallizer developed by Aeschback (1) without draft tube and baffles.
3. Survey municipal lime-soda ash water softening plants to determine the degree of uniformity of crystal habit. If scanning electron microscope examinations show uniform crystal habit, similar to that exhibited in the Lansing system, an effort to model $\text{Mg}(\text{OH})_2$ and CaCO_3 co-precipitation would be justified.

APPENDICES

APPENDIX A

A PROGRAM FOR FITTING COUNTS TO THE
SIZE INDEPENDENT GROWTH MODEL

(Counts should be made for 1 ml samples.)


```

SUBROUTINE REGRES( N,A,B,SS)
COMMON X(41),Y(20)
SXX=SYX=SYX=SY=SY=0.0

C
DO 10 I=1,N
J=2*I
SX=SX+X(J)
SY=SY+Y(I)
SYY=SYY+Y(I)*Y(I)
SYX=SYX+X(J)*Y(I)

10

C
AN=N*B=(SYX-SX*SY/AN)/(SXX-SX*SY/AN)
A=(SY-B*SX)/AN
SS=(S-Y-A*SY-B*SYX)/(AN-2.)
RETURN
END
```

APPENDIX B

METHODS OF MAGNESIUM AND
HYDROXIDE ANALYSIS

APPENDIX B

METHODS OF MAGNESIUM AND HYDROXIDE ANALYSIS

Since reactant concentrations are the independent variables of the reaction this research attempted to model, their determination was a key to success. Analysis by ion specific electrodes, conductivity and titration were all considered. The analysis methods actually used were chosen by default for the most part.

By use of a combination of conductivity and material balance, the concentrations of both hydroxide and magnesium could be measured (17, 23). Preliminary investigation of solutions containing magnesium and hydroxide showed negative deviation from theoretically predicted conductivities even at low concentrations. This could only be a result of ionic association. In order to use conductivity technique for supersaturated solutions, a series of calibration runs would have to be made involving solutions of known concentrations. In principle this could be accomplished by mixing solutions at very short residence times so that no nucleation takes place. Unfortunately, complete mixing is a function of contact time and proving that no nucleation takes

place would not be simple. Assuming mixing without nucleation could be accomplished, calibration would still be very time consuming. Using conductivity measurements to determine if the system were at steady state was discarded in an attempt to simplify crystallizer configuration when the walls were found to need periodic scraping.

Ion specific electrodes for determination of magnesium concentration are well documented in the literature (15, 29, 32) and use of the pH meter for hydroxide concentration is widespread. Electrodes and conductivity bridges have the advantage of direct measurement; no filtration as is necessary for titration techniques. Unfortunately, they are not extremely accurate; small inaccuracies become quite substantial when pH is converted to concentration. In retrospect the filtration may cause even larger errors than would be caused by these techniques. Future studies would be well advised to give direct measurement techniques a long hard look.

Titration to determine total and phenolphthaline alkalinities was used as discussed in Standard Methods (27). By definition:

$$\text{Phenolphthaline Alkalinity (P)} = 50,000 (C_{\text{CO}_3} + C_{\text{OH}})$$

$$\text{Total Alkalinity (T)} - \text{P} = 50,000 (C_{\text{HCO}_3} + C_{\text{CO}_3})$$

The dissociation product for bicarbonate (K_2)

$$K_2 = 4.6668 \times 10^{-11} = C_{\text{CO}_3} \times C_{\text{H}}/C_{\text{HCO}_3}$$

The dissociation product for water ($K_{\text{H}_2\text{O}}$)

$$K_{\text{H}_2\text{O}} = 10^{-14} = C_{\text{H}} \times C_{\text{OH}}$$

$$\text{pH} = -\log C_{\text{H}}$$

By rearrangement, a knowledge of P, T and a guess at pH will, by iteration on the following equations, give a rather accurate hydroxide concentration.

$$C_{\text{CO}_3} = (T - P)/50,000/(10^{-\text{pH}}/4.6668 \times 10^{-11} + 1)$$

$$C_{\text{OH}} = P/50,000 - C_{\text{CO}_3}$$

$$C_{\text{H}} = 10^{-14}/C_{\text{OH}}$$

$$\text{pH} = -\log C_{\text{H}}$$

Inclusion of activity coefficients has little effect on the above equations because similar coefficients cancel one another out.

Magnesium concentration was determined by titration against EDTA as described in Diehl (9). The problems encountered with these determinations are discussed under the heading Discussion.

APPENDIX C

DATA AVERAGING

APPENDIX C

DATA AVERAGING

In each run nuclei density and growth rate were measured several times. Figures 3.1 through 3.9 are plots showing the measured values and the approximate time of measurement. Due to the rather primitive electronics of the Coulter counter (model B), it took several solution samples taken over an average of 15 minutes to determine a single numbers versus length plot, from which nuclei density and growth rate were calculated. Although nuclei density is plotted here, it is simple to determine nuclei birth rate from the expression, $B^0 = n^0G$.

Average nuclei density and growth rate were calculated for each run. In the plots, the values used in the averaging are connected by lines; those not connected to the others by a line were considered suspect. The plots illustrate that growth rate is more stable than nuclei density. This observation is consistent with the results of this study, which show nucleation rate proportional to hydroxide concentration squared while growth rate is simply proportional to the hydroxide concentration. Any change in the hydroxide concentration would be more evident in the nuclei density.

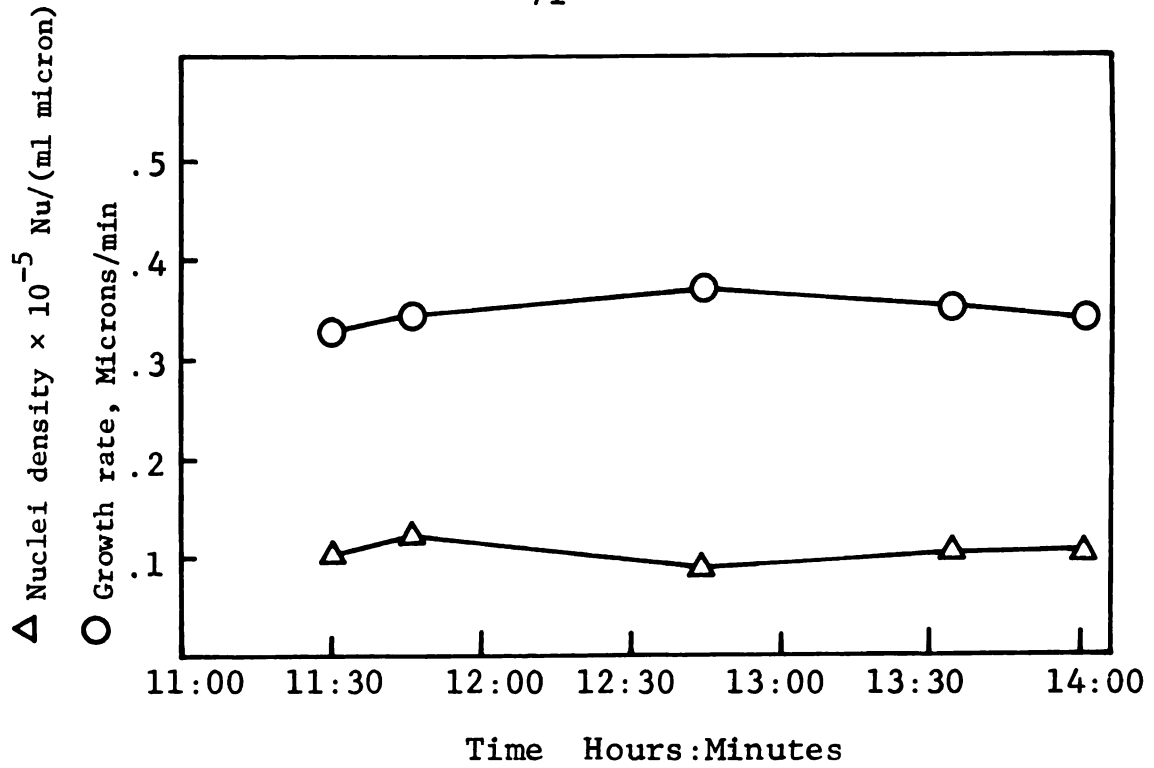


Figure C.1.--Run 5-10, started 7:55.

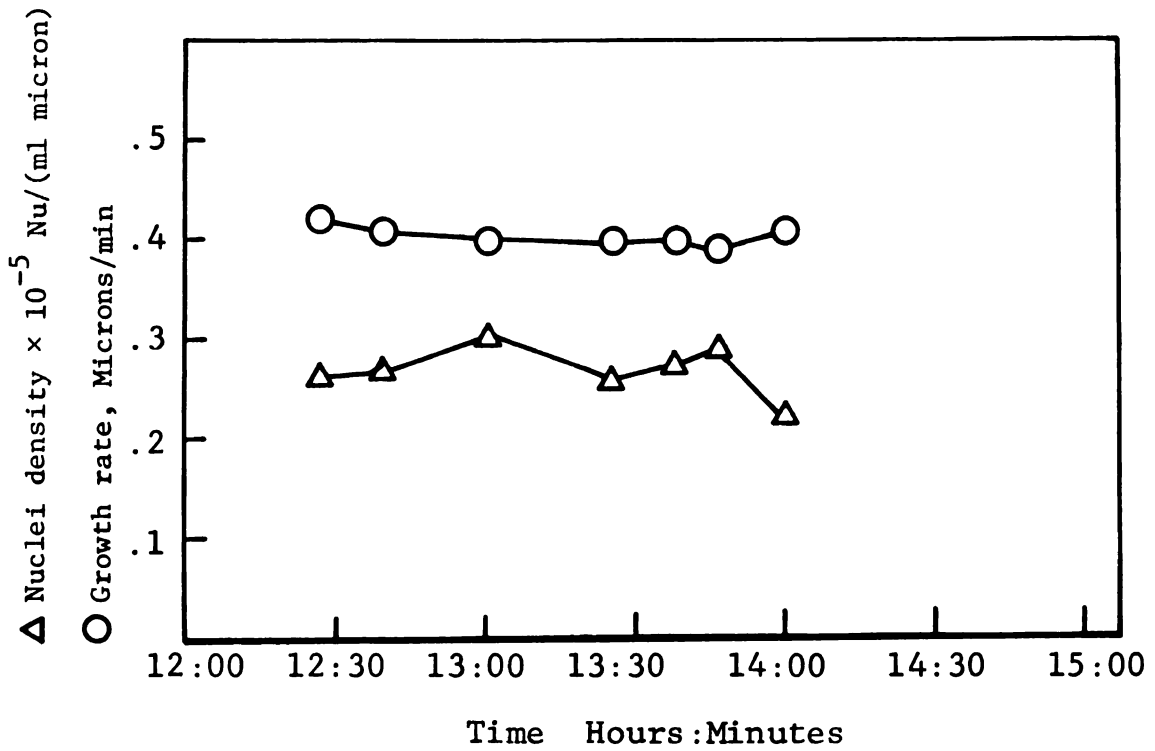


Figure C.2.--Run 5-13, started 9:30.

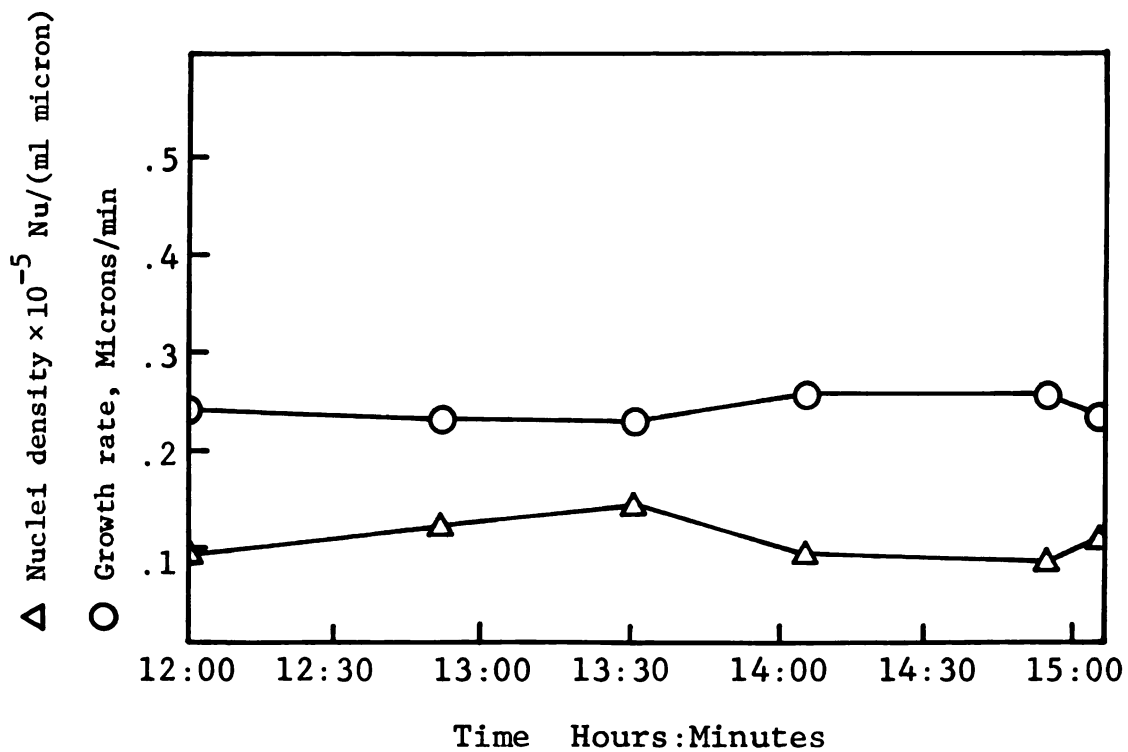


Figure C.3.--Run 5-15, started 8:20.

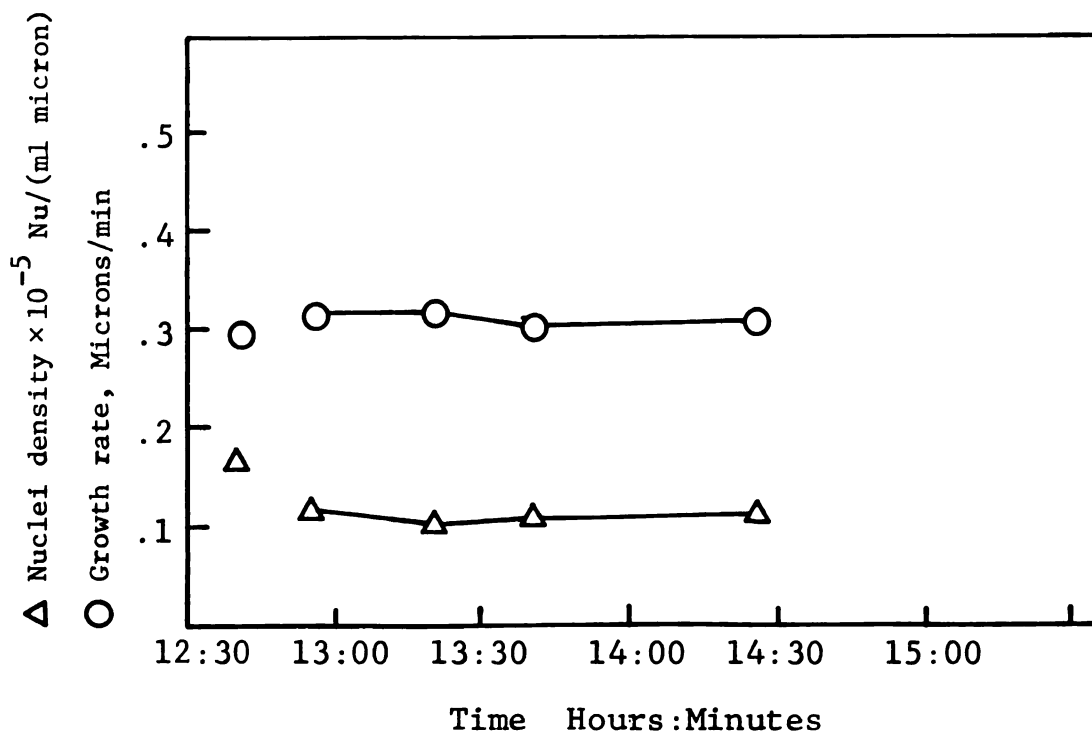


Figure C.4.--Run 5-22, started 10:20.

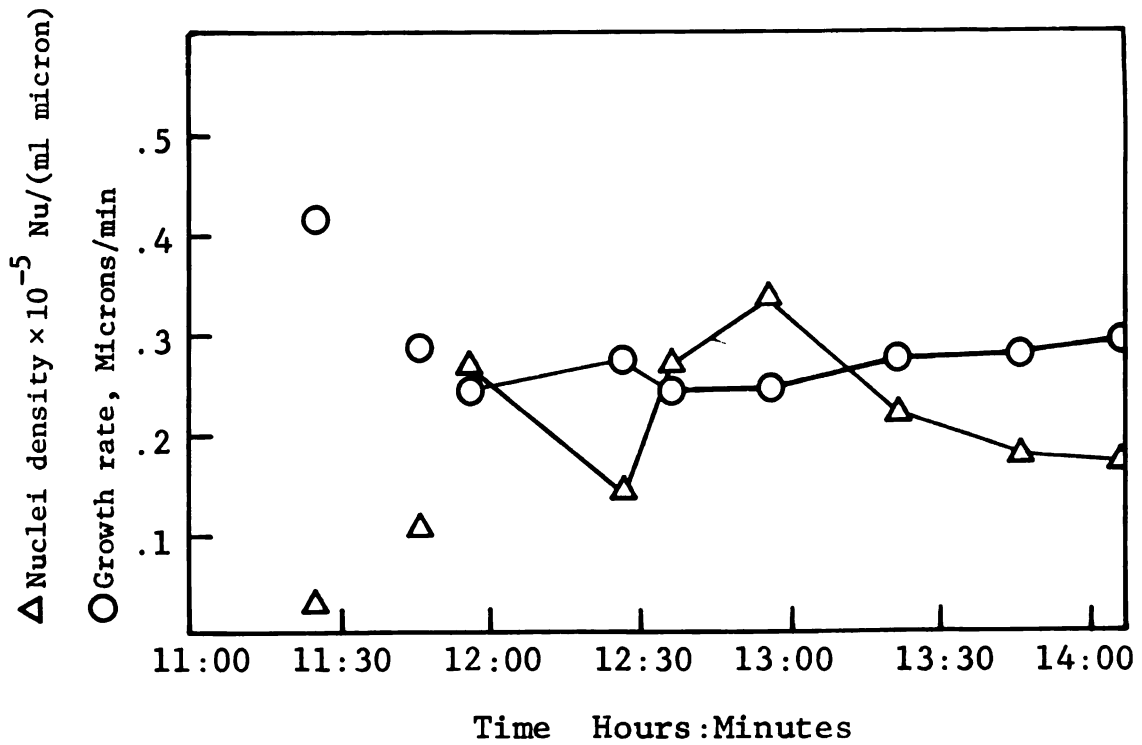


Figure C.5.--Run 5-24, started 9:00.

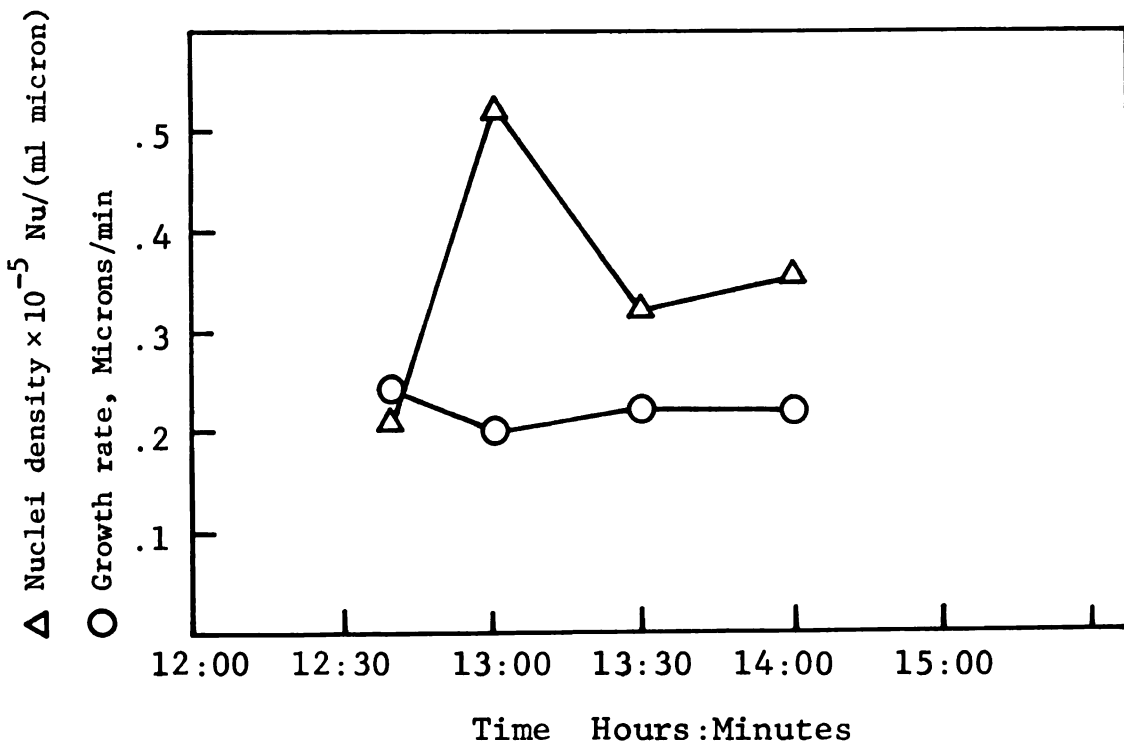


Figure C.6.--Run 5-27, started 10:00.

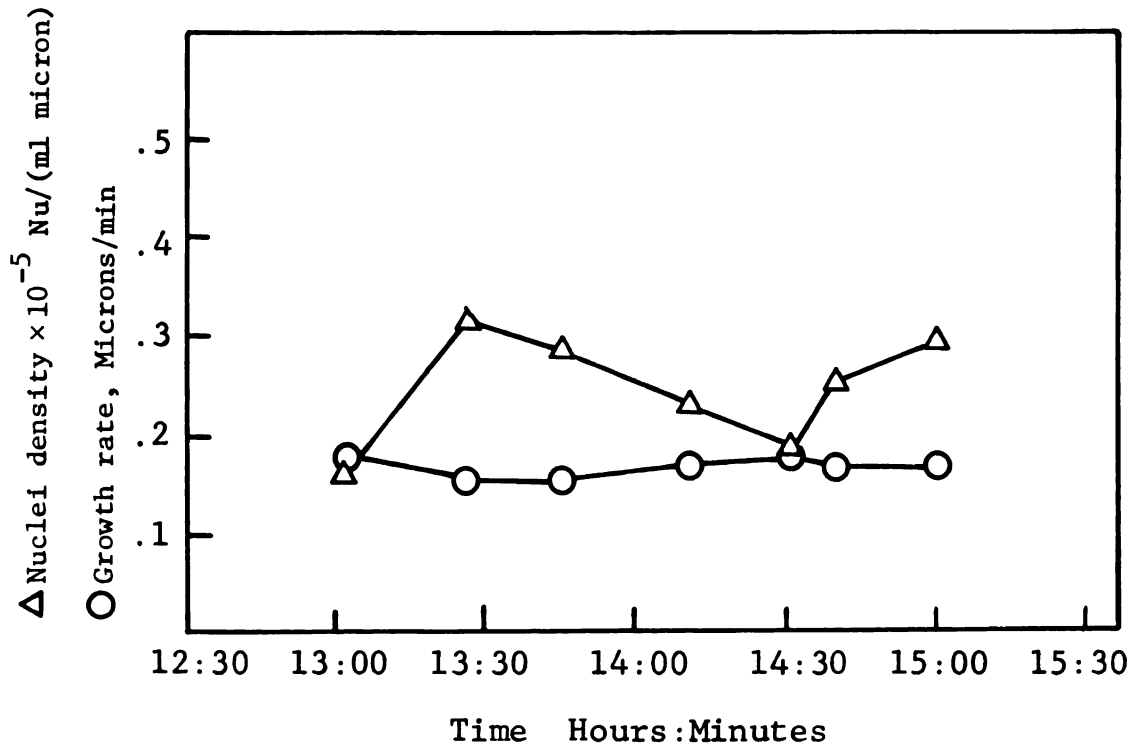


Figure C.7.--Run 6-3, started 9:15.

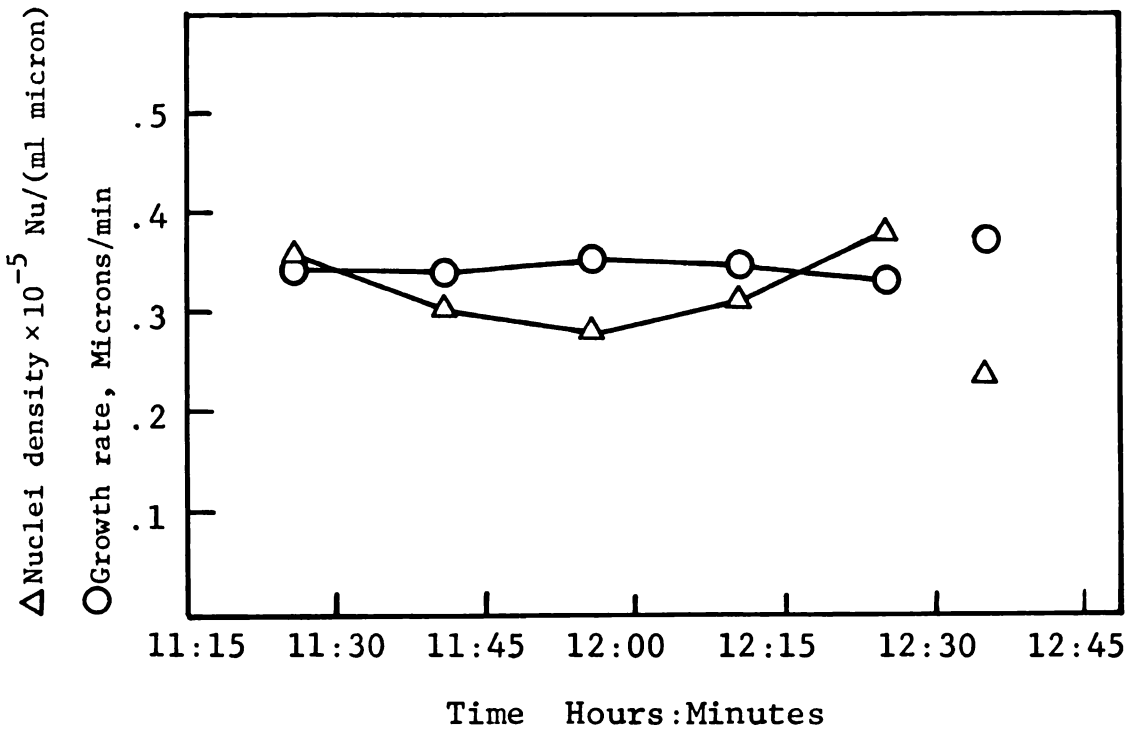


Figure C.8.--Run 6-5, started 10:07.

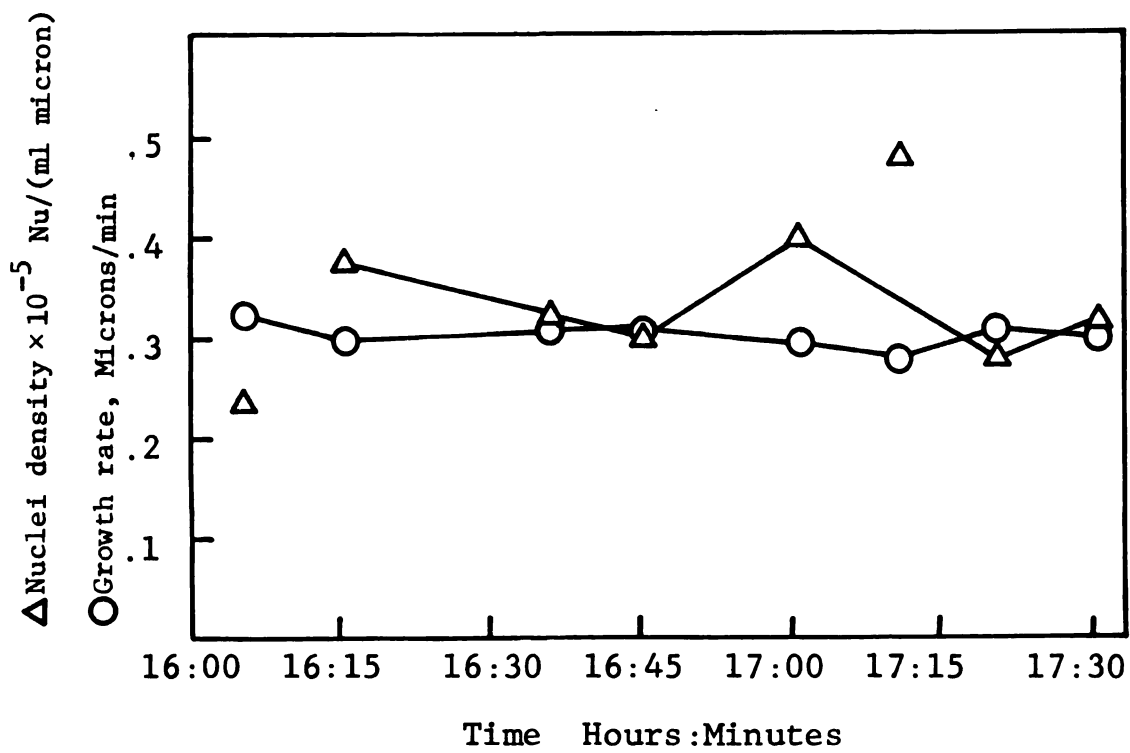


Figure C.9.--Run 6-8, started 14:25.

BIBLIOGRAPHY

BIBLIOGRAPHY

1. Aeschback, S., Attainment of homogeneous suspension in a continuous stirred tank. Chem. Eng. J., V4 N3, Dec. 1972.
2. Anshus, Byron E., On the stability of a well stirred isothermal crystallizer. Chem. Eng. Sci. V28 N2, Feb. 1973.
3. Baker, C. G. J. and Bergongnou, M. A., Precipitation of sparingly soluble salts: A model of agglomeration controlled growth. The Canadian Journal of Chemical Engineering, V52, April 1974.
4. Bauer, L. G., Contact nucleation of magnesium sulfate heptahydrate in a continuous MSMPR crystallizer. Unpublished Ph.D. thesis. Ames, Iowa, Library, Iowa State University, 1972.
5. Bendig, L. L., Contact nucleation and small crystal growth. Unpublished M.S. thesis. Ames, Iowa, Library, Iowa State University, 1974.
6. Black, Shuley, Fleming, From lime-soda softening sludges. Recovery of calcium and magnesium values. J. American Water Works Ass., V63 N10, Oct. 1971.
7. Brulhart, P. Process and plant layout considerations in the treatment of drinking water. Sulgen Tech. Rev. V52 N70, p. 45.
8. Chabereck, S, Courtney, R. C. and Martell, A. E., Magnesium Hydroxide dissociation. J. American Chemical Soc., V 74, p. 5057, 1952.
9. Diehl, H. C. Quantitative analysis. Ames, Iowa, Oakland St. Science Press, 1970.
10. Fair, G. M., Geyer, J. C. and D. A. Okum. Water and wastewater engineering. New York, N.Y., John Wiley and Sons, Inc., 1968.
11. Gunn, D. J. and Murthy, M. S. Kinetics and mechanisms of precipitations, Chemical Engineering Science, V 27, p. 1293, 1972.

12. Hartline, Ralph A., Computer analysis of cooling water blowdown reduction. Unpublished M.S. thesis, Engineering Library, Michigan State University, East Lansing, Michigan, 1975.
13. Hudson, H. E., Evaluation of plant operating and Jar-Test Data. J. American Water Works Ass., V65 N6, May 1973.
14. Judkins, J. F. and Wynne, R. H., Crystal-seed conditioning of lime-softening sludge. J. American Water Works Ass., V64, May 1972.
15. Kester, Dana and Pytkowicz, R. M., Magnesium sulfate association at 25°C in synthetic sea water. Limnology and oceanography, V13 N4, Oct. 1968.
16. Klein, David H., Homogeneous nucleation of magnesium hydroxide. Talania Rev. Int. Ed. V14 N8, 1967.
17. Loveland, J. W., Conductivity and Oscillometry, in Treatise on Analytical Chem., I.M. Kolthoff and P. J. Elving, eds. P + I, Vol. 4, Interscience Pub. div. John Wiley and Sons, New York, N.Y., 1963.
18. Moore, W. J. Physical Chemistry. Prentice-Hall, Inc., Englewood Cliffs, N.J., 1964.
19. Mullin, J. W. Crystallisation. Butterworths, London, 1972.
20. Nyvlt, J. Evaluation and characteristics of the particle size composition of products made in agitated crystallizers. Int. Chem. Eng., V9 N3, July 1969.
21. Nyvlt, J. and Mullin, M. W. Periodic behavior of continuous crystallizers. Chem. Eng. Sci. V25 N1, Jan. 1970.
22. Randolph, A. D. and Larson, M. A. Theory of Particulate Processes. Academic Press, New York, N.Y., 1971.
23. Rossum, John R., Checking the accuracy of water analysis through the use of conductivity. J. American Water Works Ass., April 1975.
24. Sawyer, C. N. and McCarty, P. L. Chemistry for Sanitary Engineers. McGraw-Hill Book Co., New York, N.Y., 1967.

25. Schierholz, Paul M., Kinetics of crystallization in a dilute system. Unpublished Ph.D. thesis, Ames, Iowa, Library, Iowa State University, 1974.
26. Schierholz, Paul M. and Stevens, John D. Determination of the kinetics of precipitation in a dilute system. Paper presented to 67th AIChE Annual Meeting, Washington, D.C., December 1-5, 1974.
27. Standard Methods for the examination of water and wastewater. American Public Health Association, Inc., New York, N.Y., 1967.
28. Strickland, Constable, R. J. Kinetics and mechanism of crystallization. Academic Press, London, 1968.
29. Thompson, Mary E., Magnesium in sea water: An electrode measurement. Science, V153, Aug. 1966.
30. Water, City of Dayton Water Department, 101 West Third Street, Dayton, Ohio 45402.
31. Water supply system, Board of Water and Light, Lansing, Michigan 48895.
32. Wood, W. W., Rapid reaction rates between water and a calcareous clay as observed by specific-ion electrodes. J. Research U.S. Geol. Survey, V1 N2, Mar.-April 1973.

MICHIGAN STATE UNIVERSITY LIBRARIES



3 1293 03084 9826

MSU LIBRARY SERVICES